Supporting Information

Thermally stable Zinc Hydride Catalyst for Hydrosilylation of CO_2 to Silyl Formate at Atmospheric Pressure

*Hassan A. Baalbaki, Julia Shu, Kudzanai Nyamayaro, Hyuk-Joon Jung, Parisa Mehrkhodavandi**

Department of Chemistry, University of British Columbia, 2036 Main Mall, Vancouver, British Columbia, V6T 1Z1, Canada.

Table of Contents

General Methods.

Unless otherwise indicated, all air- and/or mositure-sensitive reactions were carried out under dry nitrogen using MBraun glove box and standard Schlenk line techniques. NMR spectra were recorded on a Bruker Avance 300 MHz, 400 MHz. ^{1}H NMR chemical shifts are reported in ppm versus residual protons in deuterated solvents as follows: δ 7.27 $CDCl_3$, $^{13}C\{^{1}H\}$ NMR chemical shifts are reported in ppm versus residual ^{13}C in the solvent: δ 77.2 $CDCl_3$. $^{31}P\{^{1}H\}$ NMR chemical shifts are reported in ppm. X-ray diffraction measurements were carried out on a Bruker APEX DUO diffractometer equipped with graphite monochromated Mo-Kα radiation. Bruker SAINT software package1 was used to integrate images. Absorption correction was done using SADABS.[1] Structure solutions were obtained using SHELXT[2] and refined using SHELXL[3] via the Olex2 interface.[4] All non-hydrogen atoms were refined anisotropically, and all hydrogen atoms were constrained to geometrically calculated positions. Crystal Maker software was used to design the graphical representation of crystal strucutes.[5] Elemental Analysis CHN was performed using a Carlo Erba EA1108 elemental analyzer. The elemental composition of unknown samples was determined by using a calibration factor. The calibration factor was determined by analyzing a suitable certified organic standard (OAS) of a known elemental composition. Infrared spectra were recorded using a PerkinElmer Frontier IR Single-Range Spectrometer.

Materials.

Solvents (THF, pentane, toluene, hexane and diethyl ether) were collected from a Solvent Purification System from Innovative Technology, Inc. whose columns were packed with activated alumina. $CDCl_3$ and CH_2Cl_2, C_6D_6, and $C_2D_2Cl_4$ were dried over CaH_2, degassed through a series of freeze-pump-thaw cycles, and collected by vacuum distillation. Triethoxysilane and triphenylsilanol were purchased from Fischer Scientific. Diethyl zinc (1M in hexane) and trans-1,2-diaminocyclohexane were purchased from Sigma Aldrich and used without further purification. Diphenylphosphino benzaldehyde was purchased from Combi-blocks. 1L $^{13}CO_2$ cylinder was purchased from Sigma Aldrich. Dimethylanilinium Tetrakis(3,5-bis(trifluoromethyl)phenyl)borate ([$HNMe_2Ph$][BAr^F]) was generated by reacting dimethylanilinium chloride with sodium BAr^F in diethyl ether at room temperature for 4 h.[6] The

solvent was removed under high vacuum, and addition of hexane to the residual precipitated a white solid. The white solid was isolated by vacuum filtration and dried in vacuo overnight.

Characterization of second species 1-β

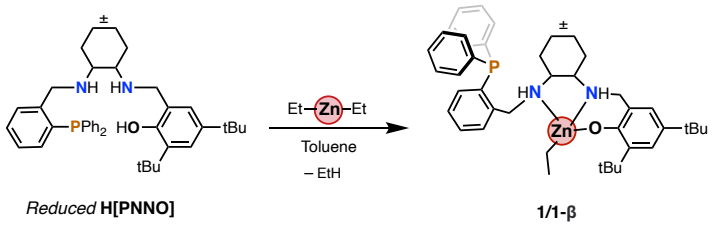

The ^{1}H NMR spectrum of **1** shows the presence of a smaller symmetric set of peaks for a second species **1-β** with the same number of signals and multiplicity as **1**. ^{31}P{^{1}H} and ^{13}C{^{1}H} NMR spectra corroborate further the presence of **1-β** (Figures S6-8). 2D COSY and HSQC NMR spectra confirm that **1-β** is also an ethyl zinc complex (Figure S11). The ratio of **1**:**1-β** was always 1:0.43. Changing the reaction time from 10 min to 5 h at 25 °C or changing the reaction solvent from toluene to THF or benzene does not change this ratio. When the (±) H[PNNO] is coordinated to zinc, multiple sources of chirality arise from the cyclohexyl ring, chiral amines, and metal center.[7] In addition, the phosphine side arm can be hemilabile and can adopt different configurations in solution which further complicates the structural analysis of the two species.[8]

To shed light on the nature of the two structures in solution, we synthesized enantiopure *RR* H[PNNO] ligand. The resulting (*RR*) alkyl zinc complex shows identical ^{1}H and ^{31}P{^{1}H} spectra to that of (±) alkyl zinc complex. This indicates that the difference between **1** and **1-β** does not rise from the stereocenters at the cyclohexene backbone.[7] We also rule out the possibility that the two isomers are a mixture of coordinated and decoordinated phosphine arm to the zinc center in solution; When reacting LZn-CH_2CH_3 with 5 eq of pyridine for 24 h, the two peaks in ^{31}P{^{1}H} slightly shift downfield but the ratio remains unchanged (Figure S16). If there is phosphine coordination, the nucleophilic pyridine should displace the labile phosphine arm due to electron saturation at the zinc center.[7, 9] Variable temperature (VT) NMR studies (D_8-Tol) from 25 to 105 °C did not result in significant changes (Figures S12-13). The ^{31}P{^{1}H} spectra shifted downfield and show that the amount of **1-β** increase slightly with increasing temperature. The ratio **1**:**1-β** was 1:0.6 at 105 °C. However, when cooling back the solution to 25 °C, the spectra were completely reversible, and the ratio restored back to its original value at 1:0.43. Also, no changes were observed when heating the same solution at 105 °C for 48 h.

We have performed NOESY experiments for complexes 1/1β and 3/3β (see new Figures S15 and.16). Since the concentrations of 1β and 3β are very low (minor complex), we were not able to figure out any geometric differences between 1 and 1β, and between 3 and 3β in solution. We did not observe any exchange coupling. Given the low concentrations of minor complexes the sensitivity of NOE will be low for them, and it is hard to differentiate between a signal and noise. Therefore, NOE experiments are not conclusive for this purpose. These observations indicate that there is no phosphine coordination to the zinc center in solution and that there is slow equilibrium between the two species.

Typical procedure for catalytic hydrosilylation of CO_2 to HCO_2-Si(OEt)$_3$

In a nitrogen-filled glovebox, of [PNNO]Zn(OSiPh$_3$) (**3**) or [PNNO]ZnH (**4**) complexes (0.021 mmol) and (EtO)$_3$Si-H (0.35 mg, 2.10 mmol) were added into a 2 ml high-pressure reactor. The reactor was sealed and taken outside the glovebox. Then, the reactor was pressurized with 1, 10 or 30 bar of CO_2, heated at different temperatures, and stirred vigorously for 24 h. Afterwards, the reactor was placed in an ice bath to cool down and excess CO_2 was vented slowly from the vessel. It should be that under these reaction conditions (EtO)$_3$SiH disproportionates into Si(OEt)$_4$ and SiH_4 . *Caution, extra care should be taken as SiH_4 gas can spontaneously ignite.*[10] The conversion of silane was determined by inverse-gated ^{13}C NMR spectroscopy (quantitative ^{13}C).[11]

DOSY NMR Spectroscopy

DOSY NMR experiments were conducted to determine the diffusion coefficients of complexes [PNNO]ZnEt **(1)**, [PNNO]Zn(OSiPh$_3$) (**3**) [PNNO]ZnH **(4)**, and [PNNO]Zn(OCOH) **(5)**. The measurements were done in C_6D_6 at 25 °C using MNOVA software. The hydrodynamic radii (r_h) were calculated using the Stokes-Einstein equation (Equation 1), in which k_B is the Boltzman constant (1.3807 X 10^{-23} J/K), D is the diffusion coefficient, and η is the viscosity of C_6D_6 (0.694 mPa s at 25 °C).[12]

$$r_h = \frac{k_B T}{6\pi\eta}$$

Equation S1. Stokes-Einstein equation to determine the hydrodynamic radii (r_h).

Table S1. Diffusion coefficients (D) and hydrodynamic radii (r_h)

Entry	Complex	D (10^{-10} m^2/sec)	log (D)	r_h (Å)
1	[PNNO]ZnEt	5.24	–9.28	6.00
2	[PNNO]Zn($OSiPh_3$)	5.15	–9.29	6.11
3	[PNNO]ZnH	5.32	–9.27	5.92
4	[PNNO]Zn(OCOH)	5.21	–9.28	6.04

Synthesis of ligand and complexes

The imino H[PNNO] ligand was synthesized according to literature without modifications[8]

Synthesis of reduced *trans* H[PNNO] ligand

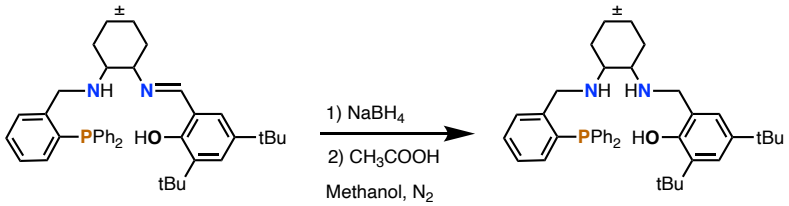

imino **H[PNNO]** **H[PNNO]**

Sodium borohydride (3.1 g, 82.0 mmol) was added slowly to a solution of H[PNNO] ligand (5.0 g, 8.2 mmol) in methanol and stirred for an hour under ice and N_2 gas. Then, acetic acid (2.3 ml, 41.0 mmol) was added dropwise and the solution at 0 °C, and the solution was allowed to warm to room temperature and stirred for 16 h under N_2. The solvent was removed *in vacuo*, and excess 4M NaOH solution was added and stirred. The solution was extracted with DCM (3 x 50 mL) and dried over anhydrous magnesium sulfate, then concentrated *in vacuo*, affording a sticky white solid. The crude solid was crystalized in a concentrated solution of acetonitrile (3.9 g, 74% yield). ^{1}H NMR (400 MHz, $CDCl_3$, 25 °C) δ 7.50 (s, 2H), 7.20-7.36 (ov m, 12H), 6.87 (s, 2H), 4.16 (d, *J* = 17.7 Hz, 1H), 3.98 (d, *J* = 13.4 Hz, 1H), 3.85 (d, *J* = 12.9 Hz, 1H), 3.76 (d, *J* = 10.7 Hz, 1H), 2.32 (s, 1H), 2.18 (M, 3H), 1.71 (M, 3H), 1.42 (s, 9H), 1.31 (s, 9H)9 1.20 (M, 3H), 0.96 (d, 1H). ^{31}P{^{1}H} NMR (121.49 MHz, $CDCl_3$, 25 °C): δ –15.85 (s). ^{13}C{^{1}H} NMR (101 MHz, $CDCl_3$, 25 °C): δ 154.92, 144.90, 144.67, 140.00, 136.97, 136.87, 136.75, 135.91, 135.77, 135.73, 134.04, 133.98, 133.85, 133.78, 133.67, 129.55, 129.14, 128.71, 128.61, 128.54, 127.37, 123.33, 122.82, 122.50, 77.26, 62.19, 60.38, 50.94, 49.61, 49.40, 34.90, 34.15, 31.76, 30.97, 29.70, 25.20, 24.60. *Elemental analysis for* $C_{40}H_{51}N_2OP$: N, 4.62; C, 79.17; H, 8.47. Found: N, 4.27; C, 78.14; H, 8.22

Synthesis of [PNNO]ZnEt **(1)**

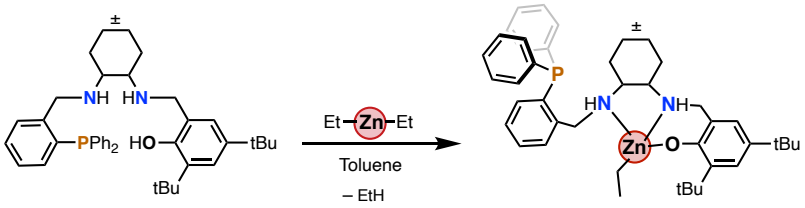

Reduced **H[PNNO]** **1/1-β**

Diethyl zinc (5.0 ml from 1M hexane, 5.0 mmol) was diluted with toluene and added dropwise to a cold solution of reduced ligand (1.0g, 1.7 mmol) in toluene (–34 ºC, 10 mL). The mixture was warmed to room temperature and stirred for 16 h. The solvent was removed *in vacuo* to yield white powder. The powder was washed with Et_2O (3×10 mL) and dried under high vacuum to yield **1** as a white solid (0.92 g, 78% yield). ^{1}H NMR (400 MHz, C_6D_6, 25 °C): δ 9.00 (m, 1H), 8.03 (s, 0.38H), 7.71 (s, 1H), 7.54-7.61 (M, 2H), 7.24-7.39 (ov m, H), 6.95-7.15 (ov M, H), 4.47 (d, 1H), 4.29 (d, 0.43H), 3.99 (m, 1.43H), 3.54 (tr, 1.45H), 3.19 (dd, 0.4H), 3.09 (m, 1H), 2.24 (m, 2jH), 2.01 (s, 9H), 1.67 (s, 4H), 1.56 (s, 9H), 1.48 (s, 4H), 1.34 (d, 4H), 1.07 (tr, 3H), 0.84 (s, 2H), 0.65 (m, 1H), 0.50 (m, 1H), 0.09 (q, 2H), -0.12 (s, 1H). ^{31}P{^{1}H} NMR (121.49 MHz, C_6D_6, 25 °C): δ –15.36 (s), –16.96 (s). ^{13}C{^{1}H} NMR (100 MHz, C_6D_6, 25 °C): δ 165.16, 164.82, 141.36, 138.39, 138.24, 134.29, 134.13, 134.09, 133.90, 133.80, 133.71, 133.60, 130.57, 129.10, 128.97, 128.90, 128.84, 128.79, 128.72, 127.99, 127.57, 124.32, 124.08, 123.85, 61.35, 60.18, 57.09, 56.15, 51.27 – 50.18 (m), 45.13, 35.48, 33.97, 32.17, 32.11, 31.54, 30.02, 29.97, 29.12, 24.87, 24.57, 13.96, 13.48, -2.04, -2.21. *Elemental analysis for $C_{42}H_{55}N_2OPZn$*: Theoretical N, 4.00; C, 72.04; H, 7.92. Found: N, 3.95; C, 71.34; H, 7.86. Single crystals suitable for X-ray analysis were grown from a solution of THF and hexane.

Synthesis of [PNNO]Zn(OSiPh$_3$) **(3)**

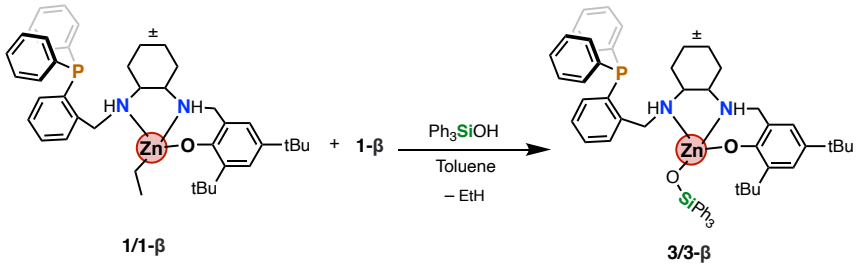

Triphenylsilanol (0.15 g, 0.53mmol) was dissolved in toluene and added dropwise to a solution of complex **1/1-β** (0.50g, 0.53 mmol) in toluene. The mixture was stirred for 16 h. The solvent was removed *in vacuo* to yield white gel. The gel was washed with Et_2O (3×10 mL) and dried under high vacuum to yield **2/2- β** as a white solid (0.42 g, 84% yield). ^{1}H NMR (400 MHz, C_6D_6, 25 °C): δ 8.96 (tr, 1H), 8.45 (m, 0.8H), 8.12 (s, 5H), 7.71 (d, 0.18), 7.57 (s, 1H), 7.49 – 7.33 (m, 1H), 7.11-7.34 (ov m, H), 6.85 – 7.08 (ov m, H), 6.82 (tr, 2H), 6.68 (s, 1H), 4.22 – 4.31 (m, 1H), 3.94 (tr, 1H), 3.84 (d, 1H), 3.64 (s, 0.17H), 3.54 (tr, 0H), 3.05 (tr, 0.17H), 3.05 (d, 0.17H), 2.92 (d, 1H),

2.19 (m, 0.16H), 2.03 (m, 0.17H), 1.85 (s, 1.5H), 1.80 (d, 1H), 1.55 (s, 9H), 1.51 (s, 2H), 1.44 (s, 9H), 1.18 (d, 2H), 0.66 – 0.61 (m, 1H), 0.48 (q, J = 12.8 Hz, 2H), 0.00 (d, J = 11.7 Hz, 1H), -0.25 (d, J = 11.5 Hz, 1H). $^{31}P\{^{1}H\}$ NMR (121.49 MHz, C_6D_6, 25 °C): –15.40 (s), –17.70 (s). $^{13}C\{^{1}H\}$ NMR (100 MHz, C_6D_6, 25 °C): δ 164.82, 142.09, 140.63, 135.49, 134.16, 133.96, 133.90, 131.19, 129.08, 129.01, 128.94, 128.84, 128.74, 128.62, 127.99, 127.57, 125.75, 123.96, 120.66, 60.88, 58.71, 57.33, 56.42, 50.11, 47.92, 35.43, 33.77, 31.99, 29.84, 29.60, 24.10. *Elemental analysis for* $C_{58}H_{65}N_2O_2PSiZn$: Theoretical N, 2.96; C, 73.59; H, 6.92. Found: N, 2.97; C, 73.43; H, 6.97. Single crystals suitable for X-ray analysis were grown from a concentrated solution of diethyl ether.

Synthesis of [PNNO]ZnH **(4)**

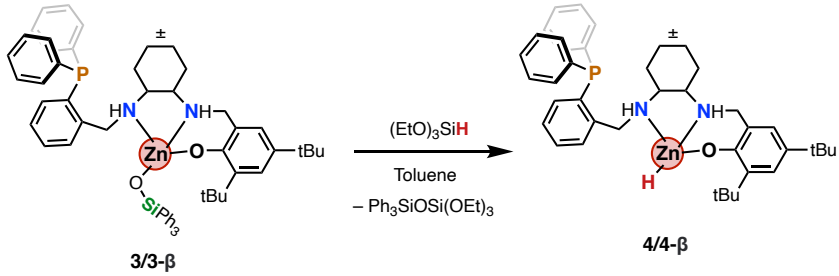

Triethoxysilane (0.12 g, 0.74 mmol) was dissolved in toluene and added dropwise to a cold solution of complex **3/3-β** (0.35g, 0.37 mmol) in toluene (–34 ºC, 10 mL). The mixture was allowed to warm to 25 °C and stirred for 16 h. The solvent was removed *in vacuo* to yield white precipitate. The precipitate was washed with Et_2O (3×10 mL) and dried under high vacuum to yield **3** as a white solid (0.16 g, 65% yield). ^{1}H NMR (400 MHz, $C_2D_2Cl_4$, 25 °C): δ 8.00 (s, 1H), 7.50 (tr, 1H), 7.33-7.45 (ov m, 12H), 7.21-7.29 (ov m, 4H), 7.10-7.18 (ov m, 3H), 6.96 (s, 0.6H), 6.83 (s, 0.6H), 6.73 (s, 1H), 6.00 (s, $C_2D_2Cl_4$), 4.66 (s, 1H), 4.53 (d, 0.6H), 4.31 (s, 2H), 3.89 (m, 2H), 3.58 (d, 2H), 2.86 (s, 0.6H), 2.17-2.45 (ov m, 1H), 2.03 (m, 0.6H), 1.89 (m, 4H), 1.78 (m, 3H), 1.46 (s, 5H), 1.30 (d, J = 14.3 Hz, 18H), 1.19 (t, J = 7.0 Hz, 0.6H), 1.08 (s, 9H), 0.27 (s, 1H). $^{31}P\{^{1}H\}$ NMR (121.49 MHz, $C_2D_2Cl_4$, 25 °C): –16.57 (s), –17.43 (s). $^{13}C\{^{1}H\}$ NMR (101 MHz, $C_2D_2Cl_4$, 25 °C): δ 162.51, 139.06 (d, J = 23.8 Hz), 138.06, 135.58 – 134.98 (m), 133.86 – 133.37 (m), 132.00, 131.35, 130.41, 129.12, 128.53, 125.37, 124.04 (d, J = 27.1 Hz), 123.13, 122.03, 120.57, 116.97 – 115.63 (m), 73.77, 73.75, 73.49, 73.22, 65.25, 60.92 (d, J = 11.6 Hz), 59.30, 57.58, 44.98, 34.63, 34.39, 33.40 (d, J = 6.5 Hz), 31.53, 31.48, 29.28, 29.21, 24.59, 24.13, 15.00.

. *Elemental analysis for* $C_{40}H_{51}N_2OPZn$: Theoretical N, 4.17; C, 71.47; H, 7.65. Found: N, 4.03; C, 69.85; H, 7.39

Synthesis of [PNNO]Zn(OCOH) **(5)**

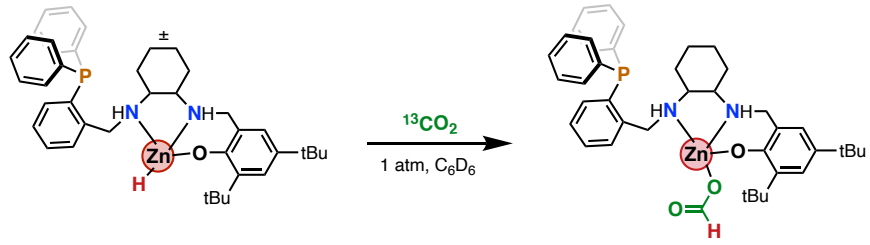

4/4-β **5/5-β**

Complex **4/4-β** was dissolved in benzene and inserted in a Teflon capped J-young tube. The tube was sealed and taken outside the glovebox. Then, the tube was frozen using liquid N_2 and connected to the Schlenk line to apply vacuum to it. After applying vacuum, the tube was subjected to $^{13}CO_2$ (from 1L cylinder that is connected also to the Schlenk line). The zinc hydride complex reacts directly with $^{13}CO_2$ to form the zinc formate. *Elemental analysis for* $C_{41}H_{51}N_2O_3PZn$: Theoretical N, 3.91; C, 68.76; H, 7.18. Found: N, 3.65; C, 67.09; H, 7.12. Single crystals suitable for X-ray analysis were grown from a concentrated solution of toluene and a layer of pentane.

Synthesis of [PNNO]ZnOH **(6)**

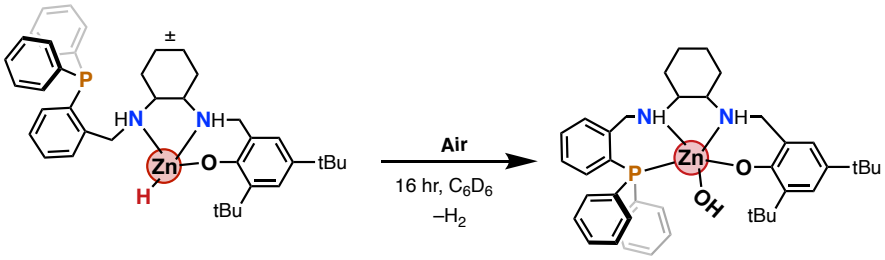

4/4-β **6**

Complex **4/4-β** was dissolved in C_6D_6 in 2 ml vial. The sample was exposed to air for 16 hr. The zinc hydride complex reacts with water vapor to form the Zn-OH complex and H_2 gas. No further purification required, and the sample was analysed as it is. ^{1}H NMR (400 MHz, C_6D_6, 25 °C): δ 11.85 (s, 1H), 7.5 (d, 1H) 7.25-7.36 (ov m, 5H), 7.12-7.18 (ov m, H), 7.00-7.12 (ov m, H), i6.98 (d, J = 2.4 Hz, 1H), 6.96 (tr, 1H), 4.02 (dd, J = 14.9 Hz, 1H), 3.83 (m, 2H), 3.59 (s, 1H), 3.00 (s, 1H), 1.96 (mi, 2H), 1.83 (m, 3H), 1.74 (s, 9H), 1.35 (s, 9H), 0.86 (m, 3H), 0.62 (m, 1H), 0.42 (m, 1H). ^{31}P{^{1}H} NMR (121.49 MHz, C_6D_6, 25 °C): –14.80 (s). ^{13}C{^{1}H} NMR (100 MHz, C_6D_6, 25 °C): δ 155.50, 145.23, 144.99, 139.90, 137.46, 137.37, 136.19, 136.04, 135.88, 134.04, 134.00,

133.90, 133.84, 133.80, 129.50, 129.45, 129.01, 128.57, 128.53, 128.50, 123.71, 122.81, 122.37, 61.86, 59.77, 51.08, 49.35, 49.15, 35.05, 34.01, 31.72, 31.29, 30.75, 29.80, 24.95, 24.38.

Synthesis of [(PNNO)Zn][BAr^F] (**2**)

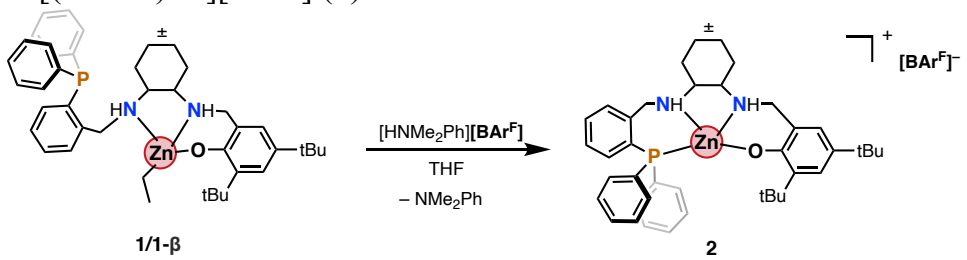

A 20 mL scintillation vial was charged with complex **1/1-β** (0.20 g, 0.29 mmol) in THF (3 ml). [HNMe$_2$Ph][BAr^F 24] (0.29 g, 0.29 mmol) in THF (2 ml) was added to the stirring solution of **1/1-β**. The reaction mixture was stirred for 4 h at r.t. The solvent was removed in vacuo to obtain a white residue and cold hexane (3 ml) was added to the residue. After stirring for 1 h, the supernatant was decanted off to remove the by-product NMe$_2$Ph. This step was repeated at least 3 times until a white solid precipitate formed. The product was washed with hexane (2 × 3 ml) and dried under high vacuum. ^{1}H NMR (400 MHz, $CDCl_3$, 25 °C): δ 7.92 – 7.81 (m, 2H), 7.77 (s, 8H), 7.70 (dd, *J* = 7.4, 1.9 Hz, 1H), 7.63 (m, 3H), 7.55 (s, 5H), 7.34 (m, *2*H), 7.11 (tr, 1H), 6.89 (s, 1H), 4.61 (d, *J* = 12.2 Hz, 1H), 3.97 (s, 2H), 3.73 (s, 1H), 2.69 (s, 1H), 2.47 (s, 3H), 2.05 (s, 1H), 1.94 (s, 1H), 1.74 (s, 3H), 1.32 (s, 18H), 1.09 (s, 4H). ^{31}P{^{1}H} NMR (121.49 MHz, $CDCl_3$, 25 °C): –14.34 (s). ^{3}C{^{1}H} NMR (100 MHz, $CDCl_3$, 25 °C): δ 162.48, 161.98, 161.49, 160.99, 138.89, 138.60, 136.44, 136.30, 134.83, 134.69, 134.65, 134.55, 133.54, 133.52, 133.46, 133.43, 133.39, 133.34, 133.25, 133.12, 133.02, 130.98, 130.91, 130.64, 130.53, 130.47, 130.35, 129.13, 129.10, 129.07, 129.04, 128.82, 128.79, 128.76, 128.73, 128.64, 128.44, 126.58, 125.93, 125.55, 123.22, 122.66, 122.02, 121.53, 120.51, 119.19, 117.56, 117.52, 117.48, 77.23, 61.31, 57.61, 50.68, 50.45, 35.17, 34.68, 34.02, 31.63, 31.61, 30.16, 29.94, 29.09, 25.29, 23.96, 23.67, 22.67, 14.11, 11.42. *Elemental analysis for* $C_{72}H_{62}BF_{24}N_2OPZn$: Theoretical N, 1.74; C, 57.49; H, 4.76. Found: N, 1.85; C, 56.88; H, 4.77.

NMR spectra of complexes

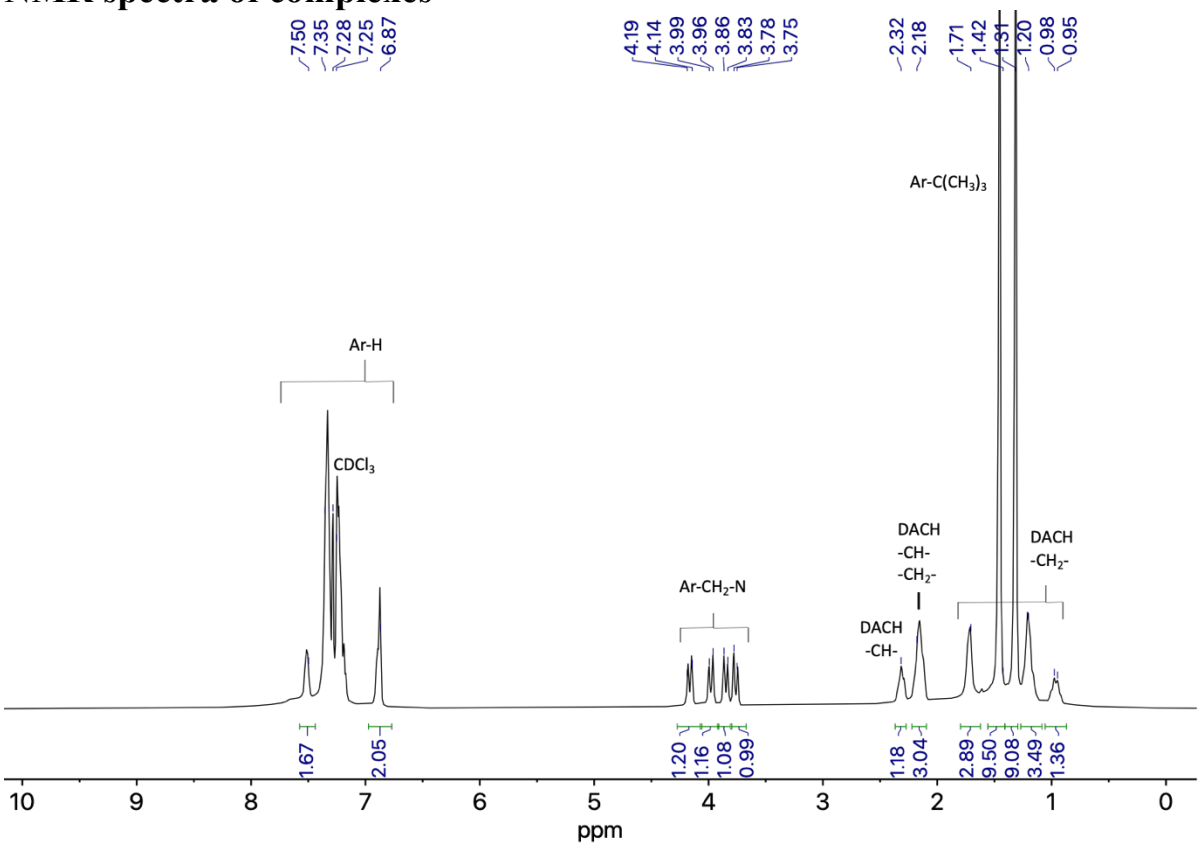

Figure S1. ^{1}H NMR spectrum of reduced H[PNNO] ligand (400 MHz, $CDCl_3$ 25 °C).

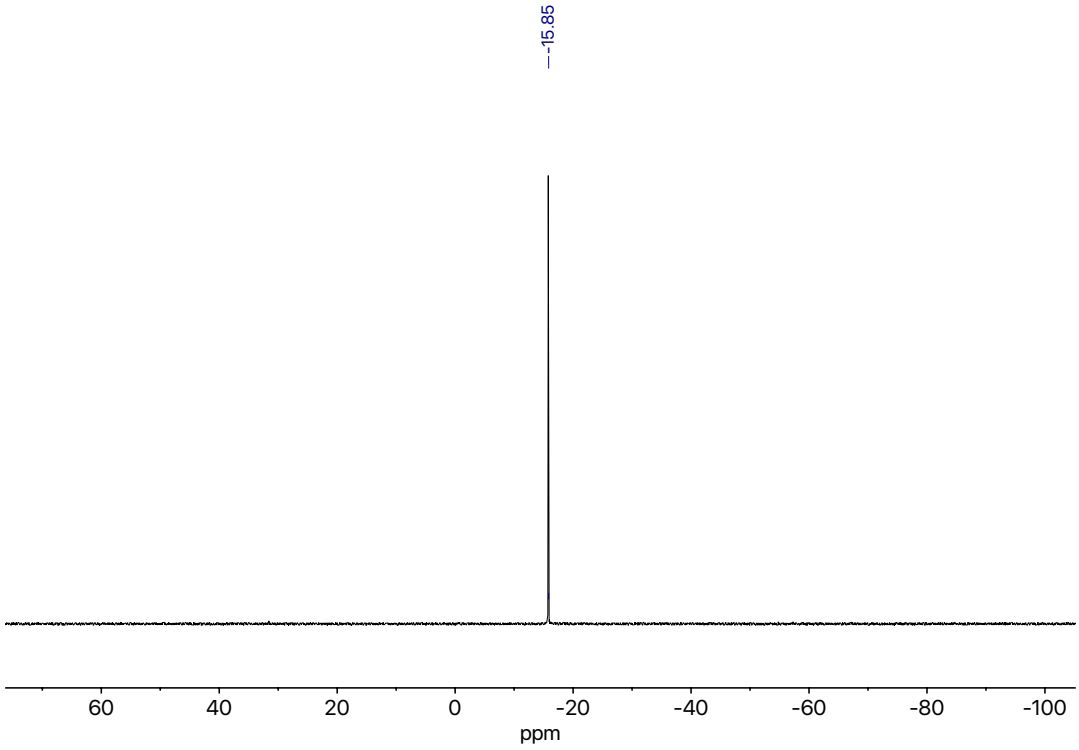

Figure S2. $^{31}P\{^{1}H\}$ NMR spectrum of reduced H[PNNO] ligand (162 MHz, $CDCl_3$, 25 °C).

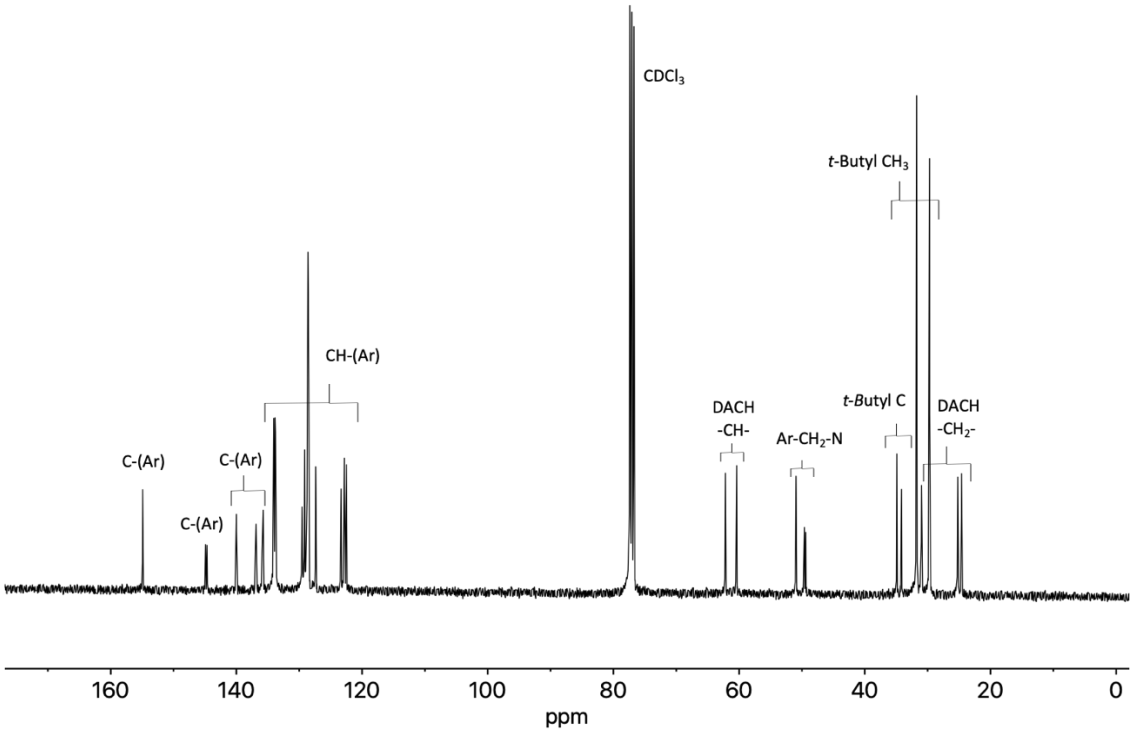

Figure S3. $^{13}C\{^{1}H\}$ NMR spectrum of reduced H[PNNO] (100.6 MHz, $CDCl_3$, 25 °C).

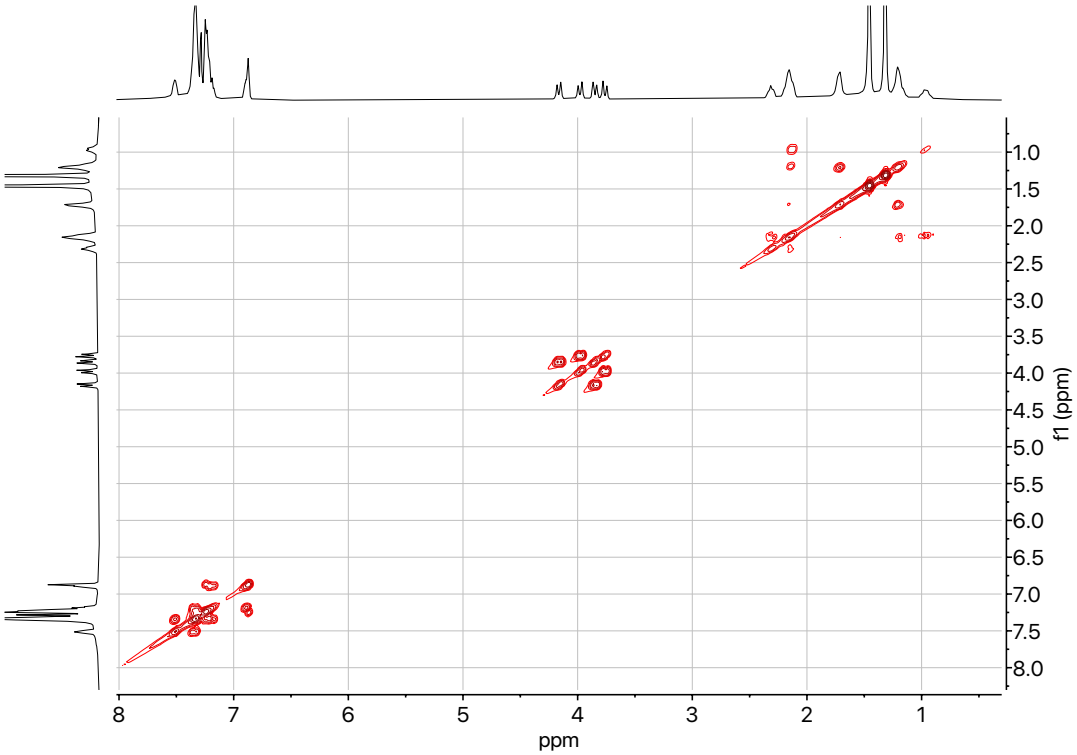

Figure S4. 2D ^{1}H-^{1}H COSY NMR spectrum of reduced H[PNNO] (400 MHz, $CDCl_3$, 25 °C).

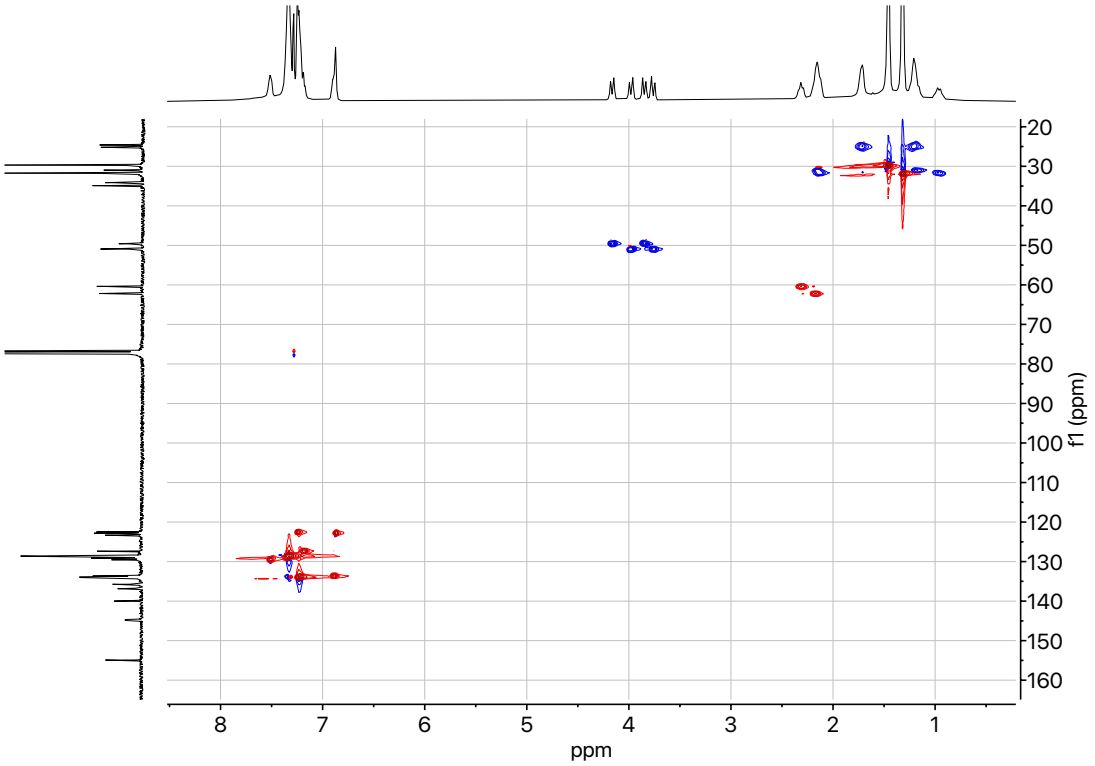

Figure S5. 2D ^{1}H-^{13}C Heteronuclear Single Quantum Coherence (HSQC) NMR spectrum of reduced H[PNNO] ($CDCl_3$,25 °C).

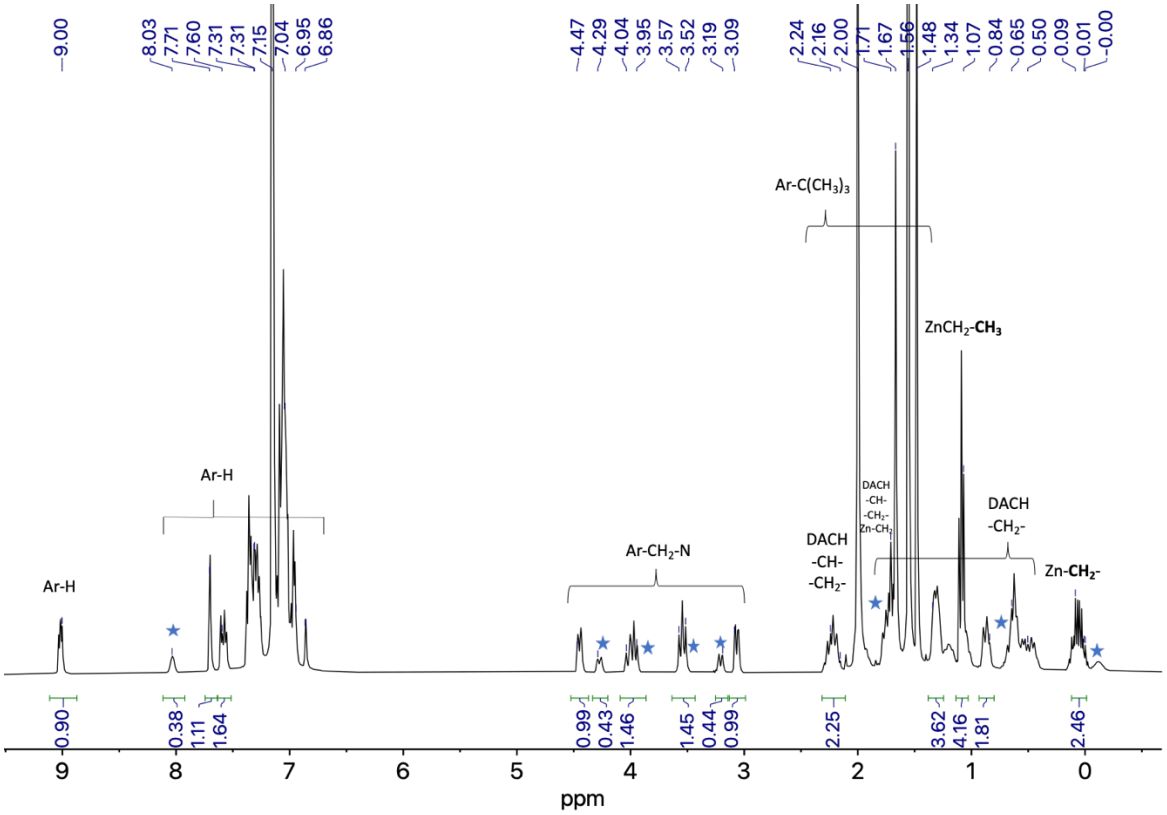

Figure S6. ^{1}H NMR spectrum of [PNNO]ZnEt **(1)** (400 MHz, C_6D_6, 25 °C). Blue stars denote a second species present in solution.

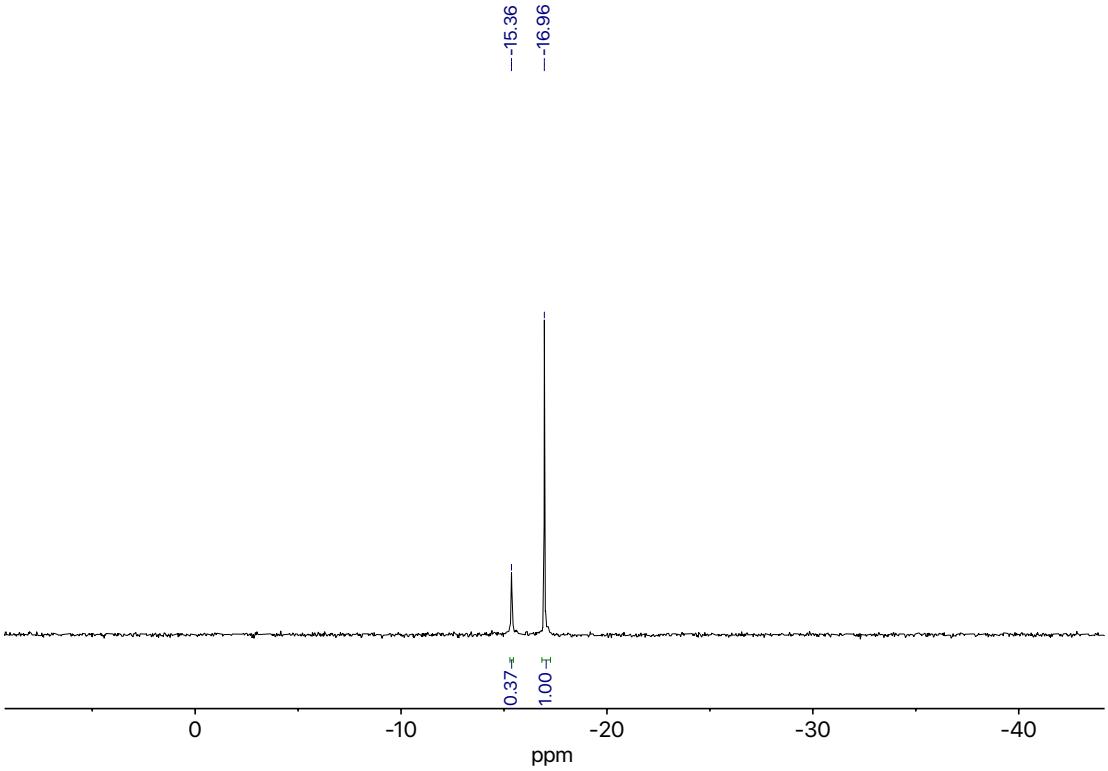

Figure S7. $^{31}P\{^{1}H\}$ NMR spectrum of [PNNO]ZnEt **(1)** (162 MHz, C_6D_6, 25 °C). Blue star denotes a second species present in solution.

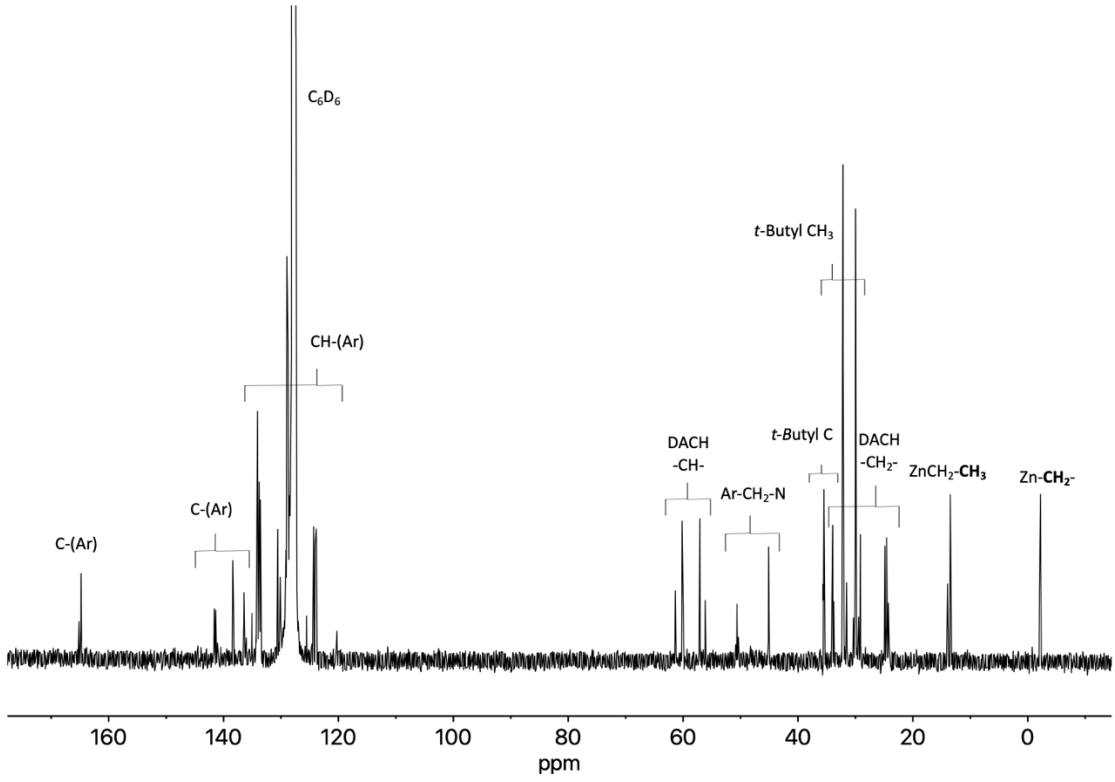

Figure S8. $^{13}C\{^{1}H\}$ NMR spectrum of [PNNO]ZnEt **(1)** (101 MHz, C_6D_6, 25 °C).

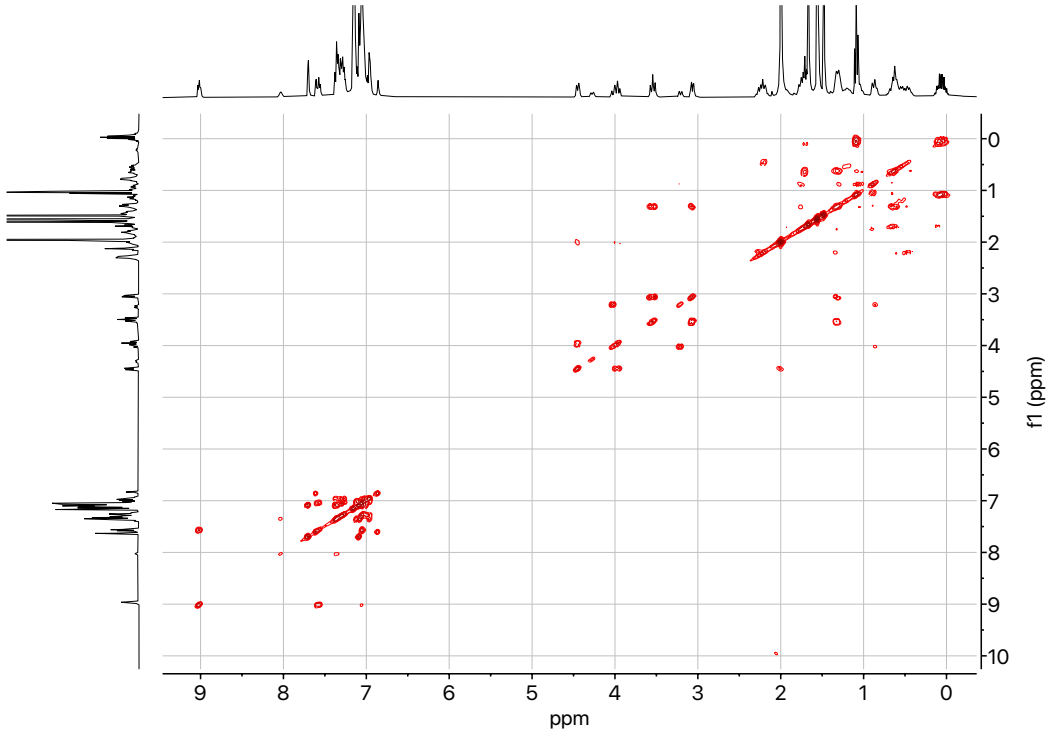

Figure S9. 2D ^{1}H-^{1}H COSY NMR spectrum of [PNNO]ZnEt **(1)** (400 MHz, C_6D_6, 25 °C)

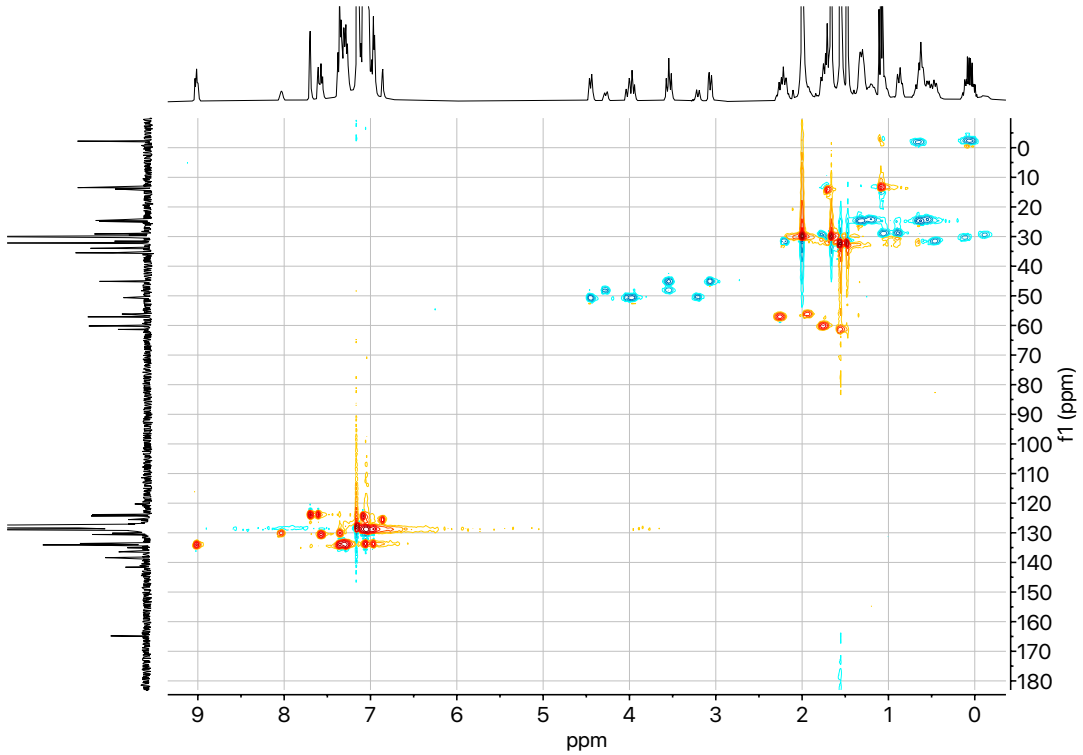

Figure S10. 2D ^{1}H-^{13}C Heteronuclear Single Quantum Coherence (HSQC) NMR spectrum of [PNNO]ZnEt **(1)** (C_6D_6, 25 °C).

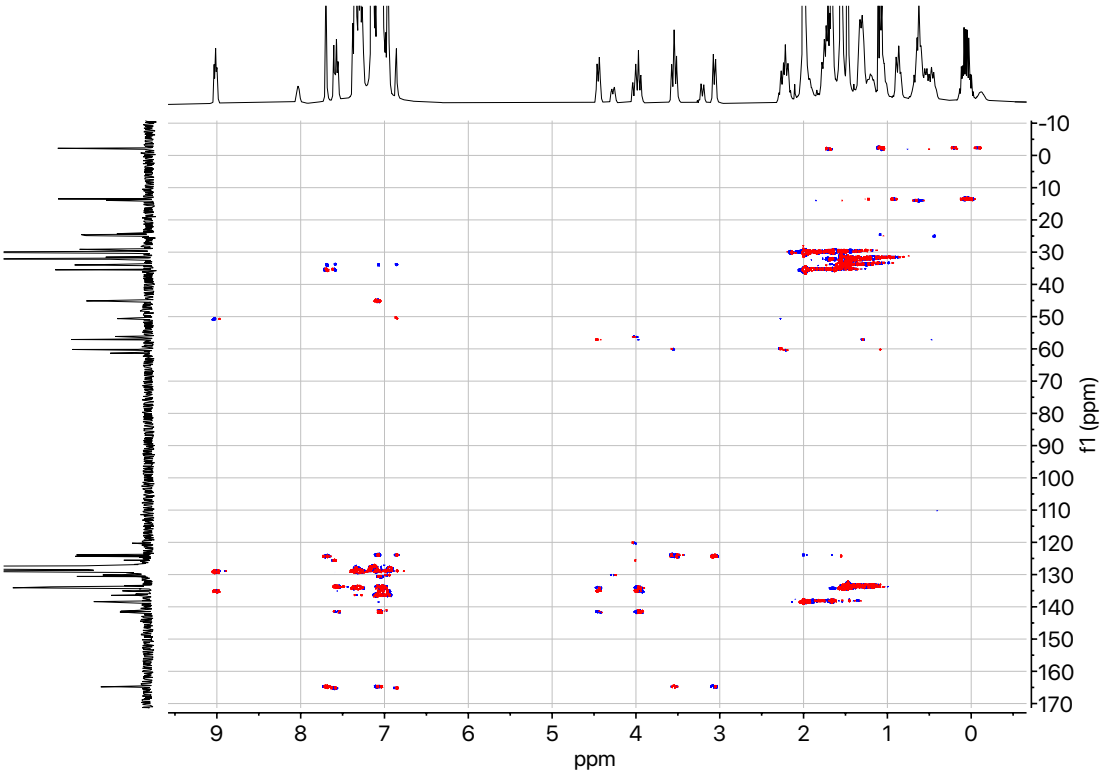

Figure S10. 2D ^{1}H-^{13}C Heteronuclear Multiple Bond Correlation (HMBC) NMR spectrum of [PNNO]ZnEt **(1)** (C_6D_6, 25 °C).

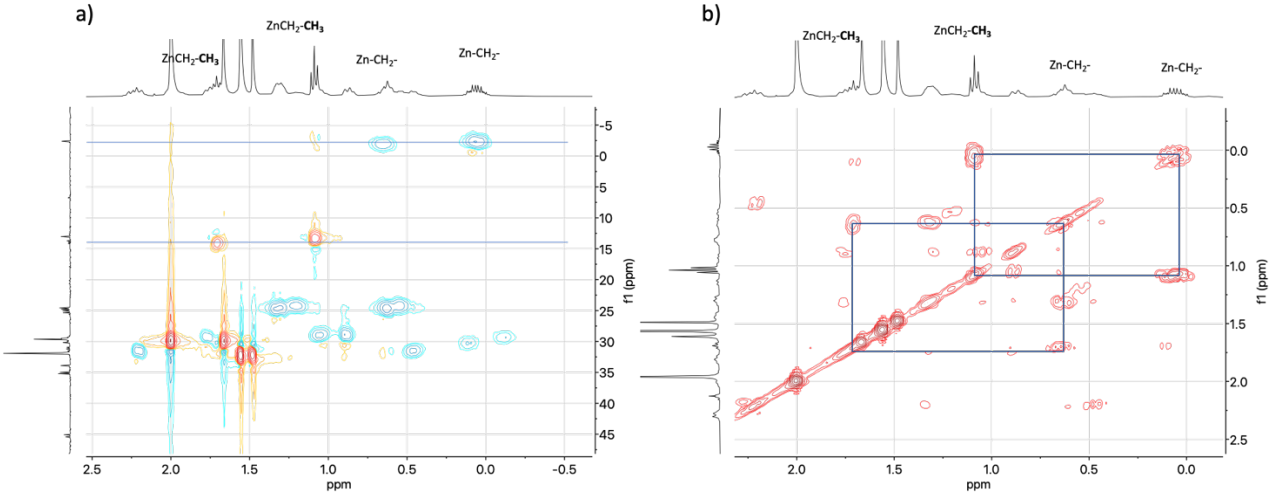

Figure S11. a) zoomed-in HSCQ spectrum. b) zoomed-in COSY spectrum to highlight the two different alkyl zinc isomers formed in solution

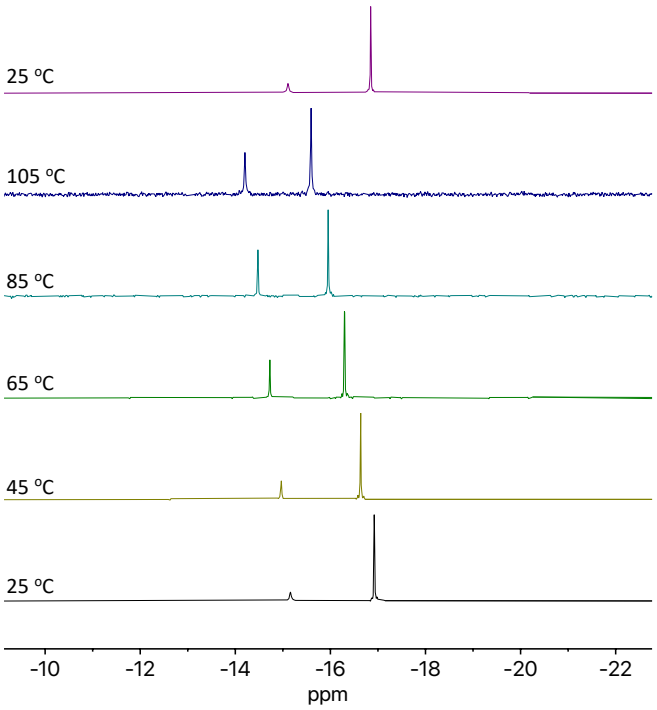

Figure S12. Variable Temperature (VT) $^{31}P\{^{1}H\}$ NMR spectra of [PNNO]ZnEt **(1)** (from 25-105 °C, and from 105-25 °C) (162 MHz, D_8-Toluene).

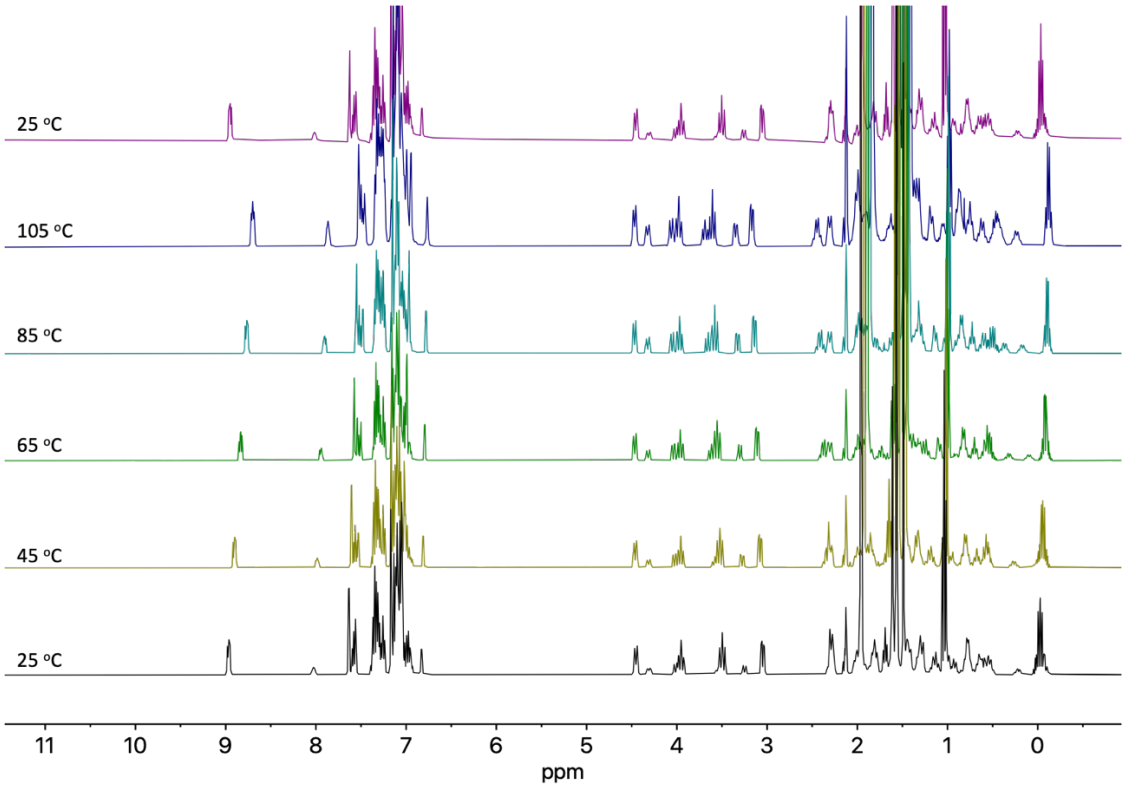

Figure S13. Variable Temperature (VT) ^{1}H NMR spectra of [PNNO]ZnEt **(1)** (from 25-105 °C, and from 105-25 °C) (400 MHz, D_8-Toluene).

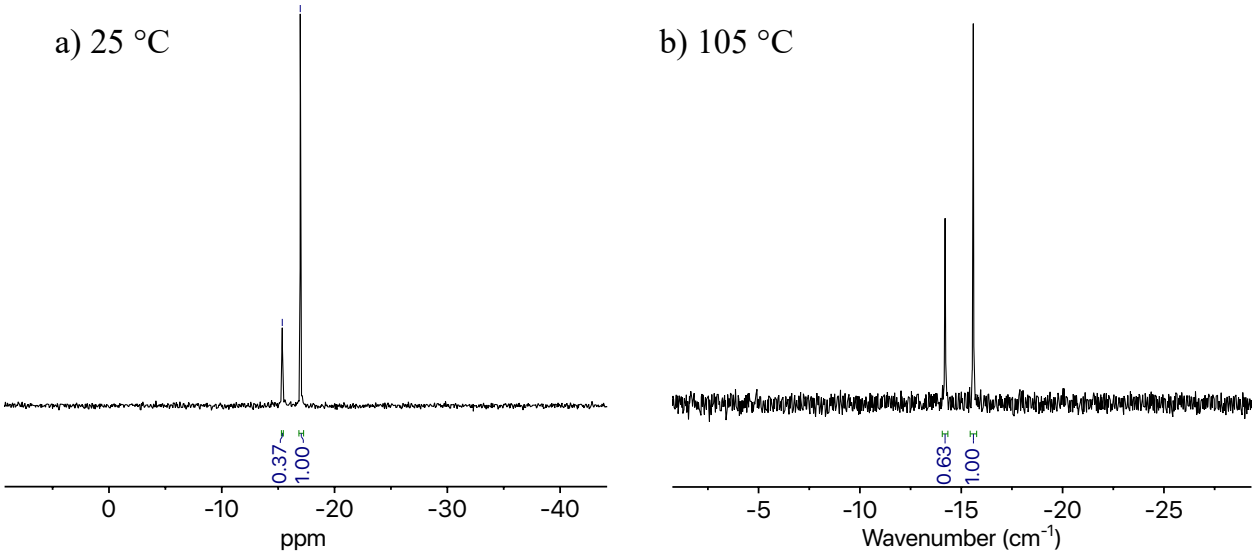

Figure S14. Separate $^{13}P\{^{1}H\}$ NMR spectra of **1/1β** at a) 25 °C; b) 105 °C

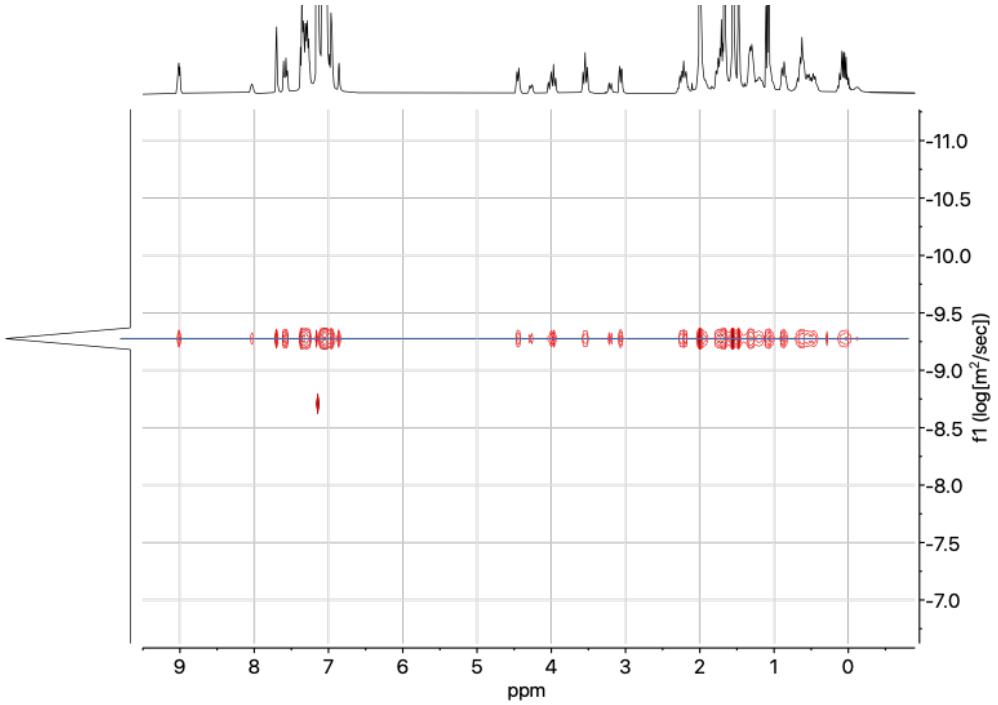

Figure S15. ^{1}H DOSY NMR spectrum of [PNNO]ZnEt **(1)** in C_6D_6 at 25 °C. The diffusion coefficient is –9.28 log(m^2/sec) or 5.24*10^{-10} m^2/sec, r_h= 6.00 Å.

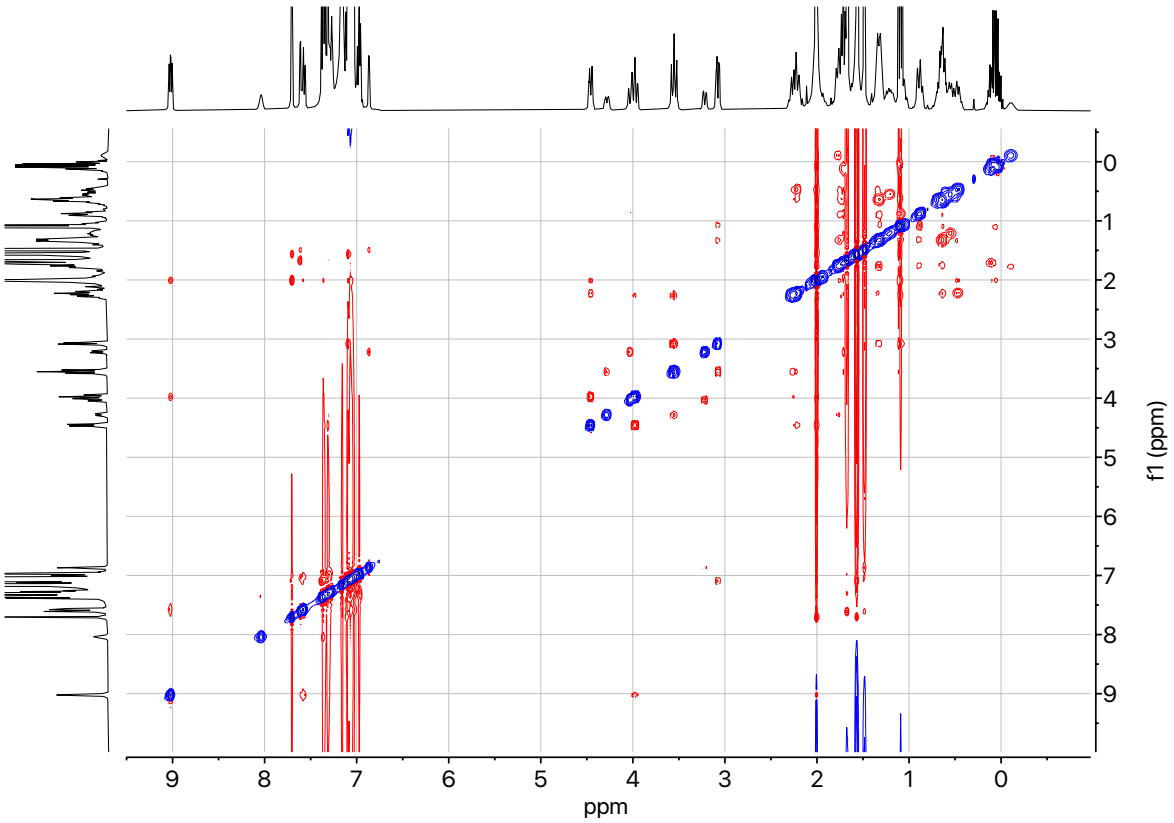

Figure S16. 2D NOESY NMR spectrum of [PNNO]ZnEt **(1)** in C_6D_6 at 25 °C.

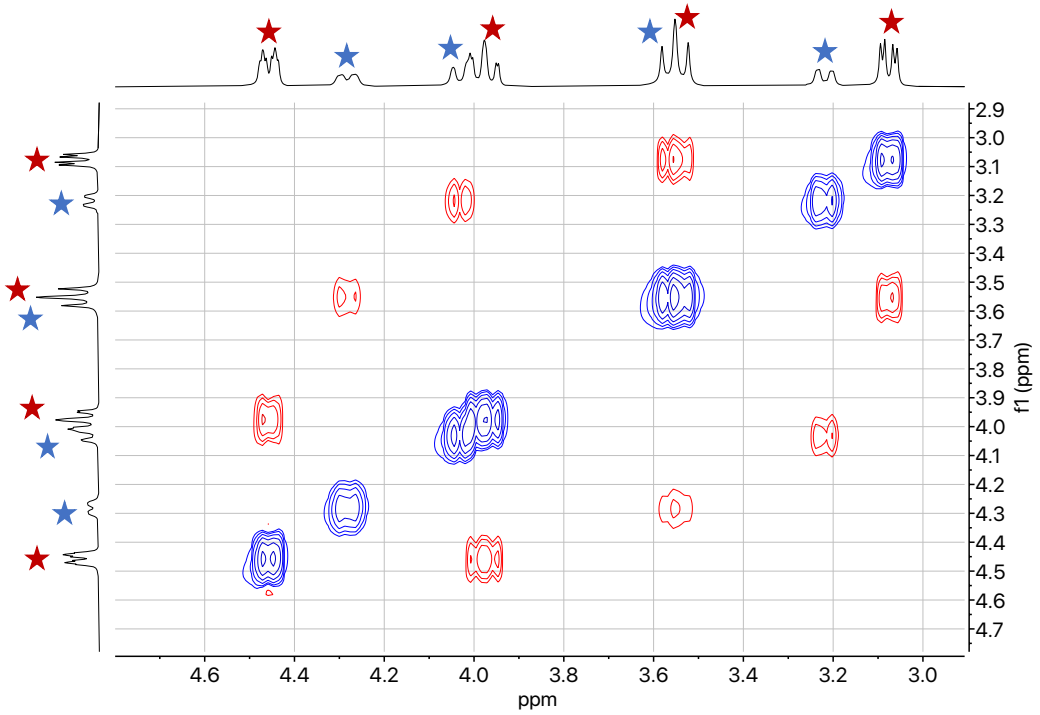

Figure S17. Zoomed-in NOSY NMR spectrum of of [PNNO]ZnEt **(1/1β)** in C_6D_6 at 25 °C. Red star denotes major isomer. Blue star denotes minor isomer.The spectrum shows that there is no exchange coupling between the two isomers.

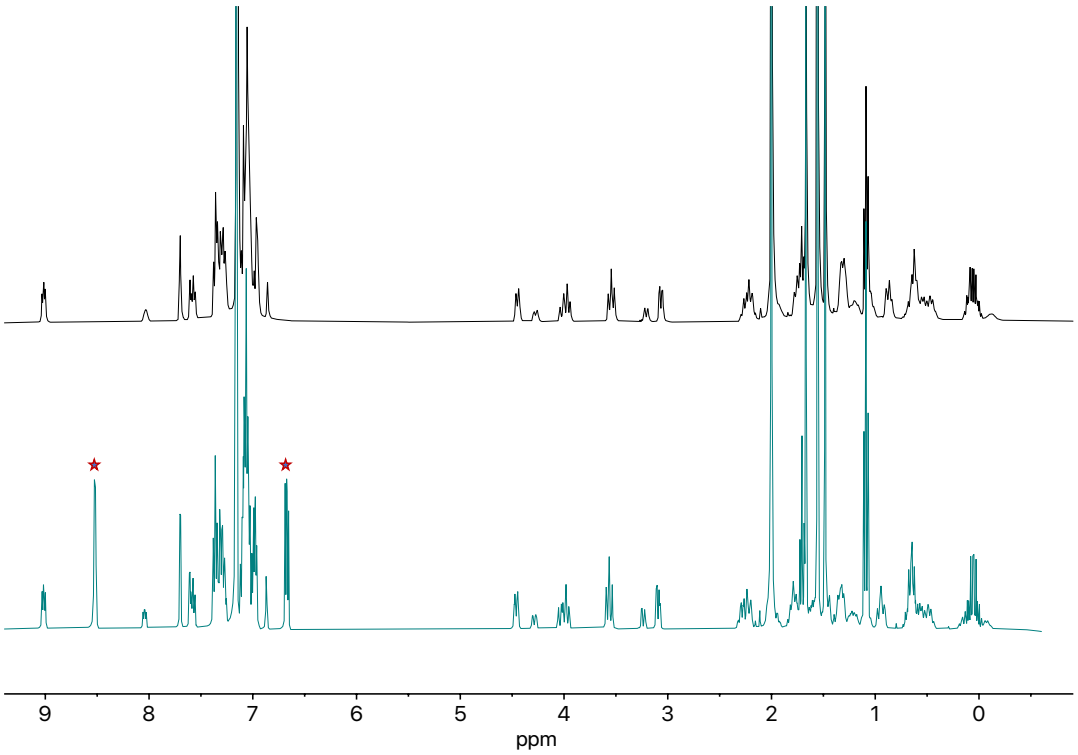

Figure S18. Overlapping ^{1}H NMR spectra (C_6D_6 at 25 °C) of alkyl zinc (top) and alkyl zinc with 3 equiv. of pyridine (bottom). Red stars denote the pyridine peaks.

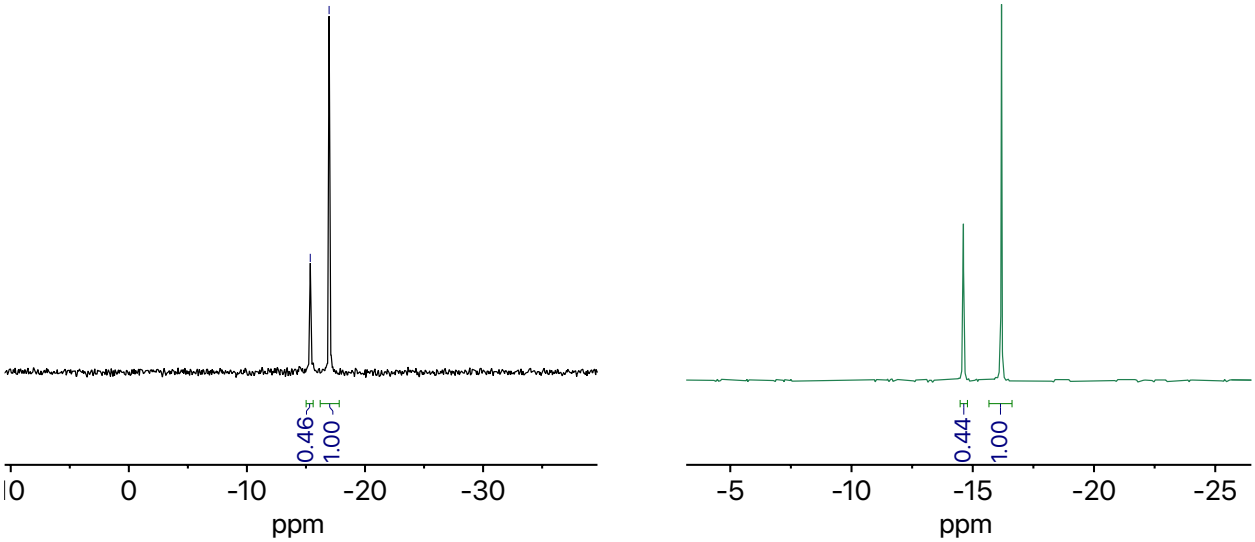

Figure S19. $^{31}P\{1H\}$ NMR spectra (C_6D_6 at 25 °C) of alkyl zinc (left) and alkyl zinc with 3 equiv. of pyridine (right).

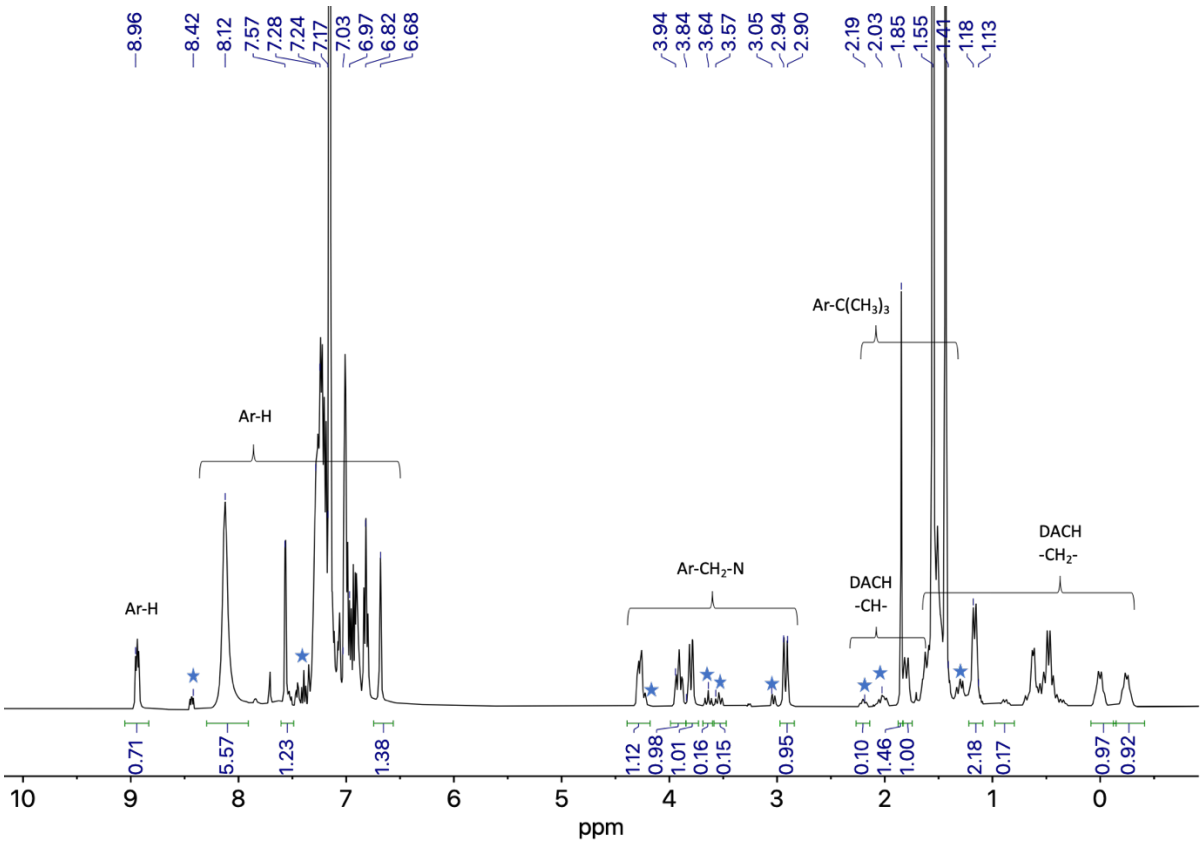

Figure S20. ^{1}H NMR spectrum of [PNNO]Zn(OSiPh$_3$) **(3)** (400 MHz, C_6D_6, 25 °C). Blue stars denote a second species present in solution

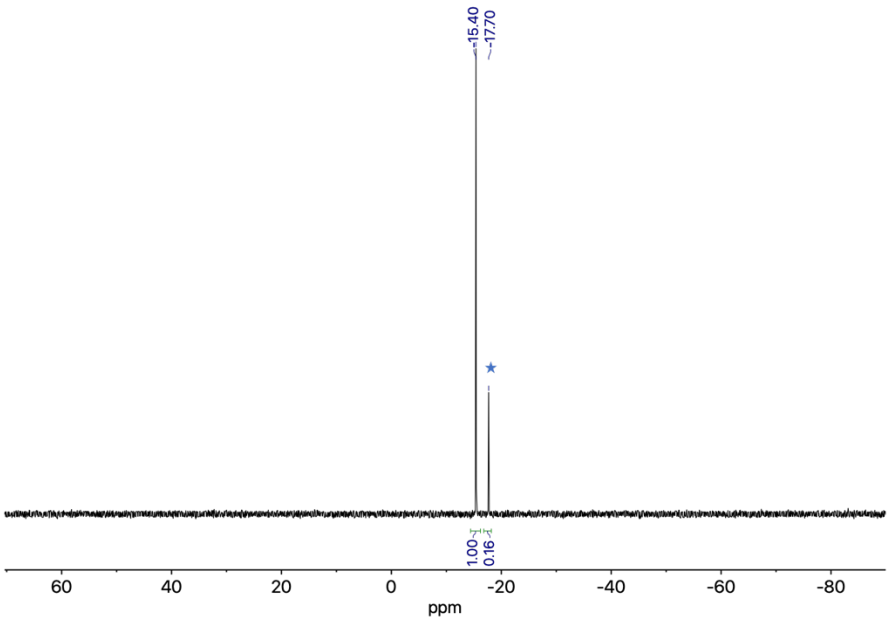

Figure **S21.** ^{31}P{^{1}H} NMR spectrum of [PNNO]Zn(OSiPh$_3$) **(3)** (162 MHz, C_6D_6, 25 °C). Blue star denotes a second species present in solution.

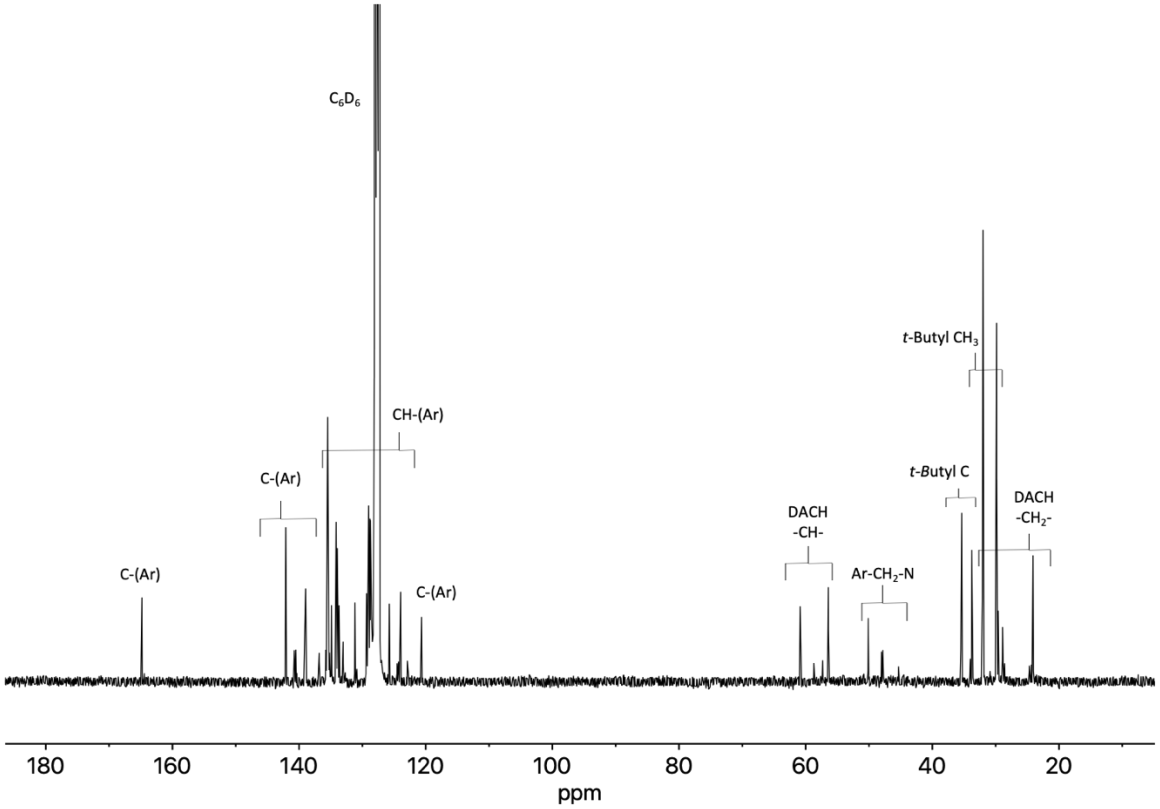

Figure S22. $^{13}C\{^{1}H\}$ NMR spectrum of [PNNO]Zn(OSiPh$_3$) **(3)** (101 MHz, C_6D_6, 25 °C).

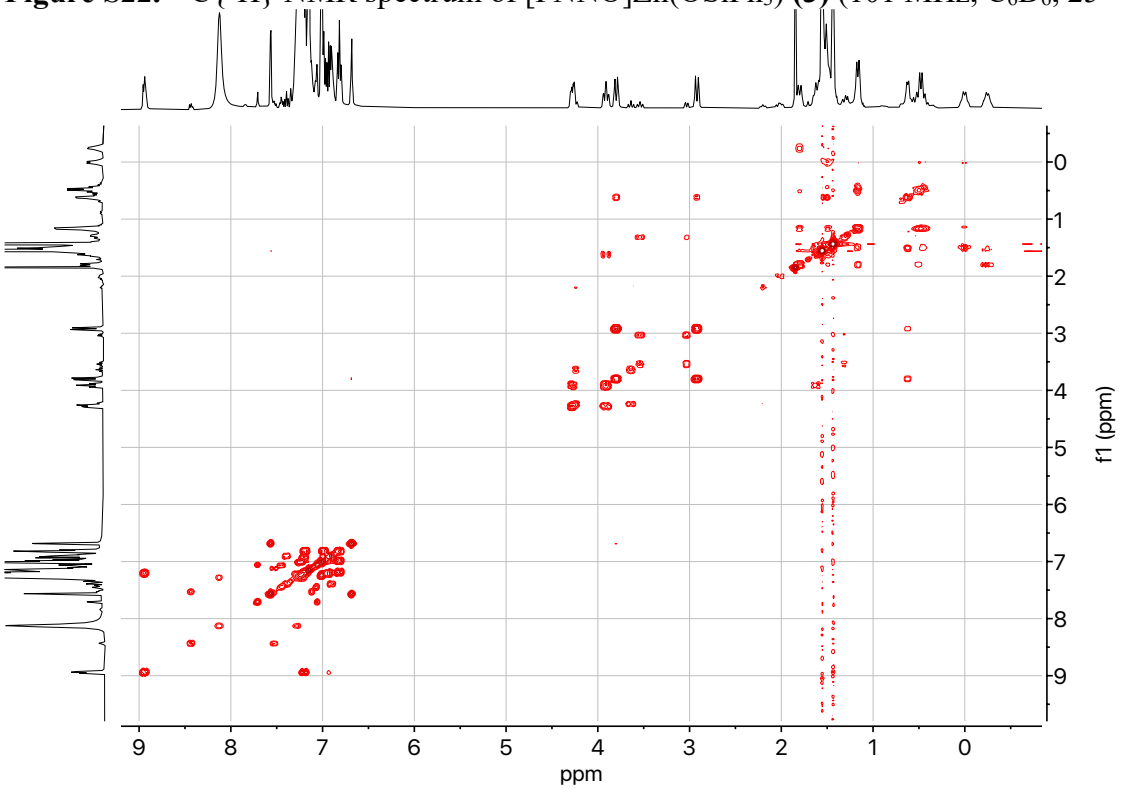

Figure S23. 2D ^{1}H-^{1}H COSY NMR spectrum of [PNNO]Zn(OSiPh$_3$) **(3)** (400 MHz, C_6D_6, 25 °C).

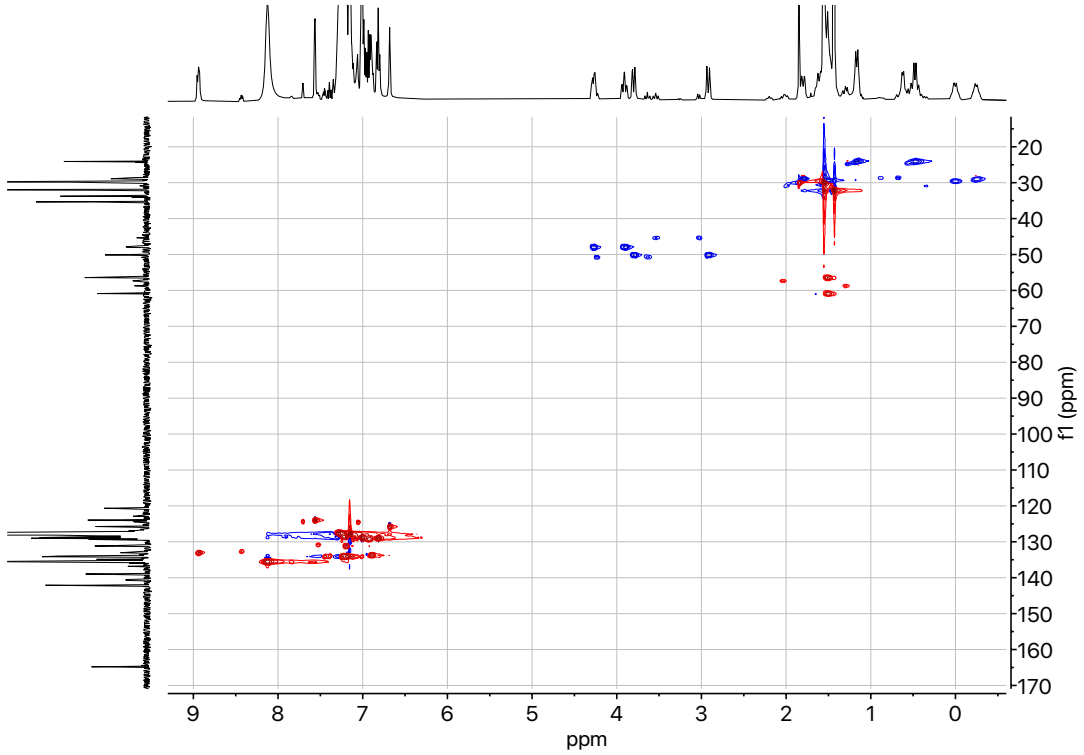

Figure S24. 2D ^{1}H-^{13}C Heteronuclear Single Quantum Coherence (HSQC) NMR spectrum of [PNNO]Zn(OSiPh$_3$) **(3)** (C_6D_6, 25 °C).

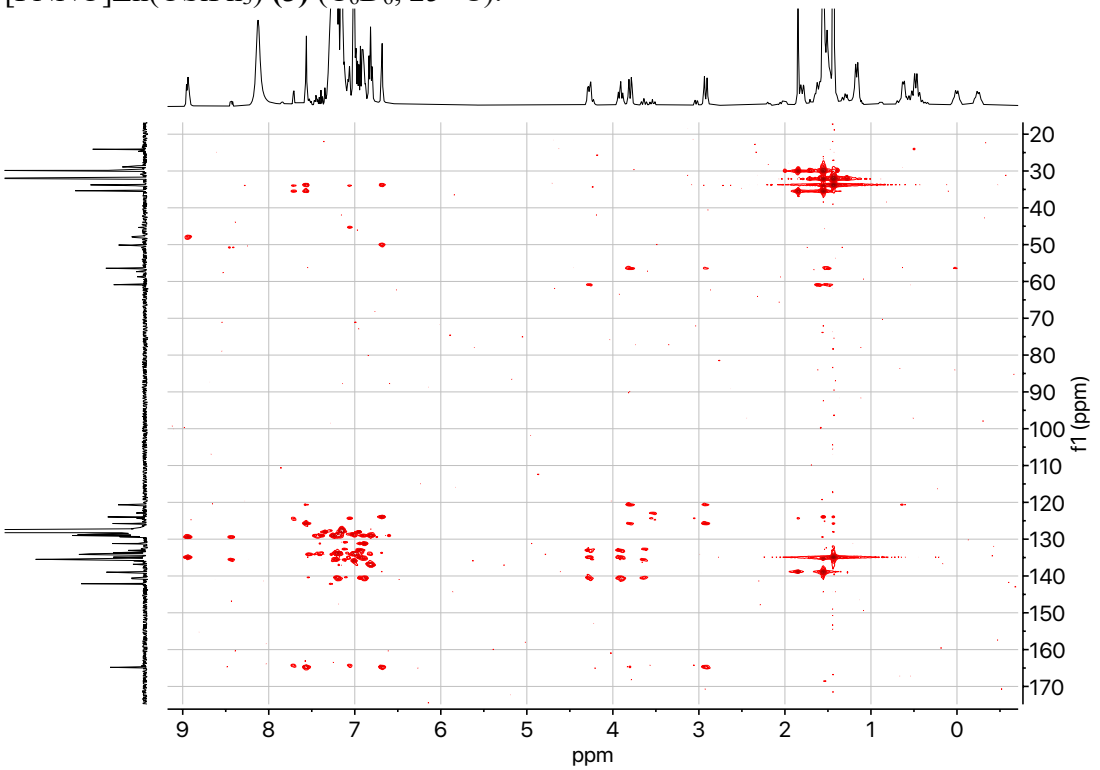

Figure S25. 2D ^{1}H-^{13}C Heteronuclear Multiple Bond Correlation (HMBC) NMR spectrum of [PNNO]Zn(OSiPh$_3$) **(3)** (C_6D_6, 25 °C).

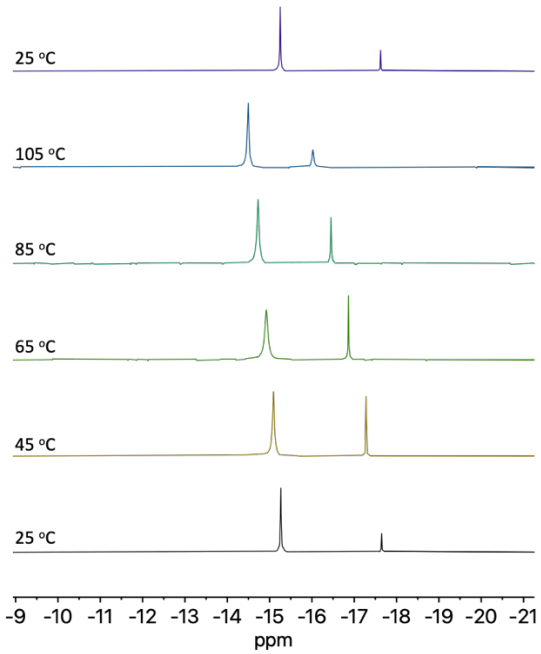

Figure S26. Variable Temperature (VT) $^{31}P\{^{1}H\}$ NMR spectra of [PNNO]Zn(OSiPh$_3$) **(3)** (from 25-105 °C, and from 105-25 °C) (162 MHz, D$_8$-Toluene).

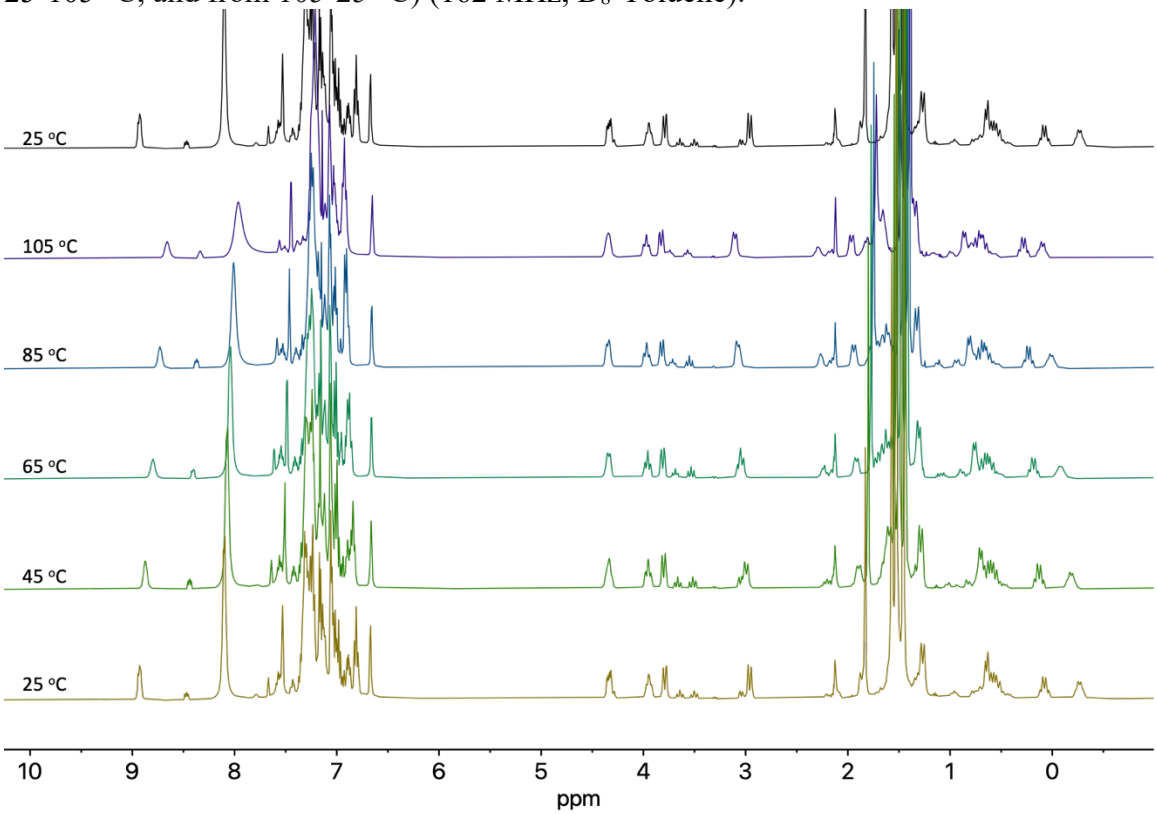

Figure S27. Variable Temperature (VT) ^{1}H NMR spectra of [PNNO]Zn(OSiPh$_3$) **(3)** (from 25-105 °C, and from 105-25 °C) (400 MHz, D$_8$-Toluene).

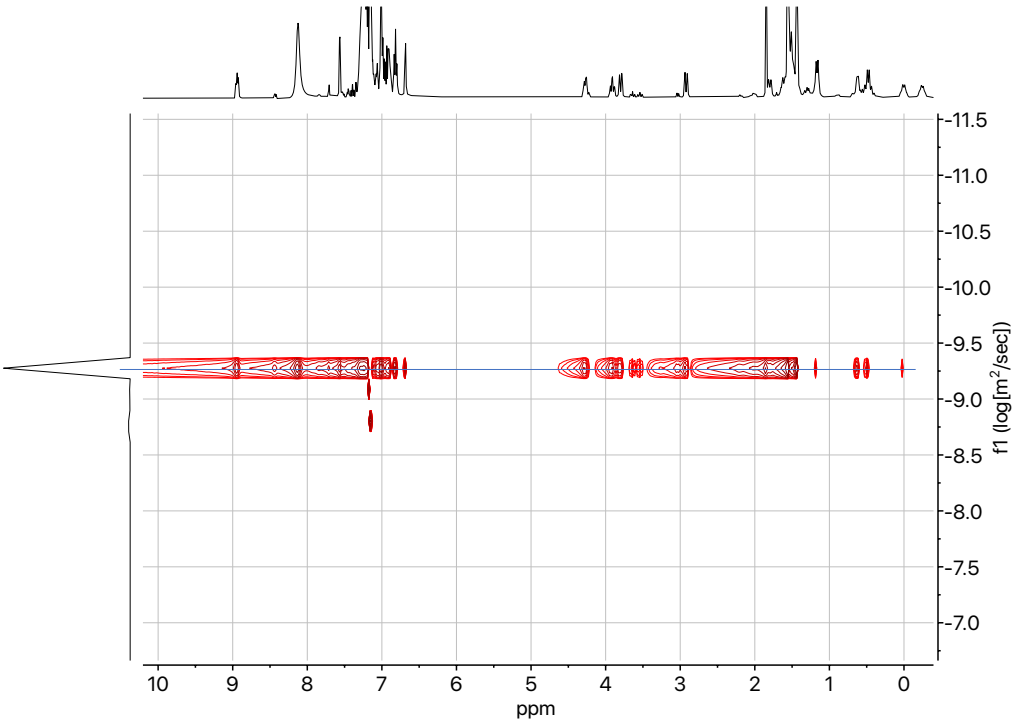

Figure 28. ^{1}H DOSY NMR spectrum of [PNNO]Zn(OSiPh$_3$) **(3)** in C_6D_6 at 25 °C. The diffusion coefficient is –9.29 log(m^2/sec) or 5.15*10^{-10} m^2/sec, r_h= 6.11 Å.

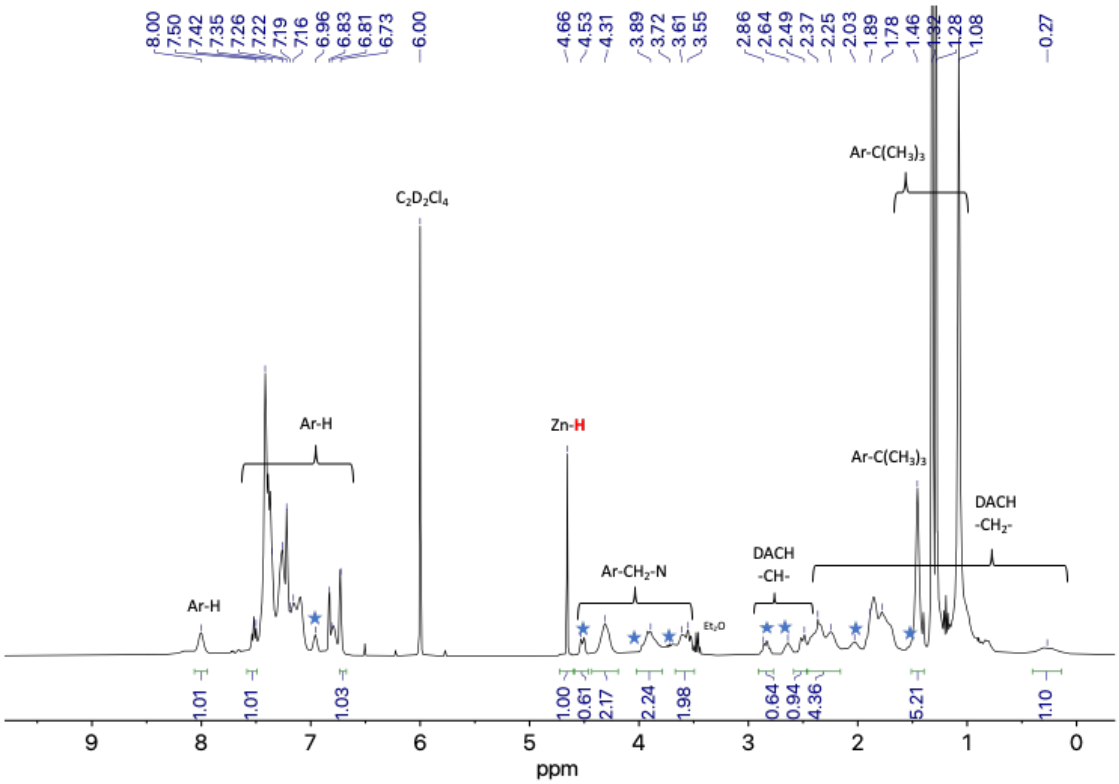

Figure S29. ^{1}H NMR spectrum of [PNNO]Zn*H* **(4)** (400 MHz, $C_2D_2Cl_4$, 25 °C). Blue stars denote a second species present in solution

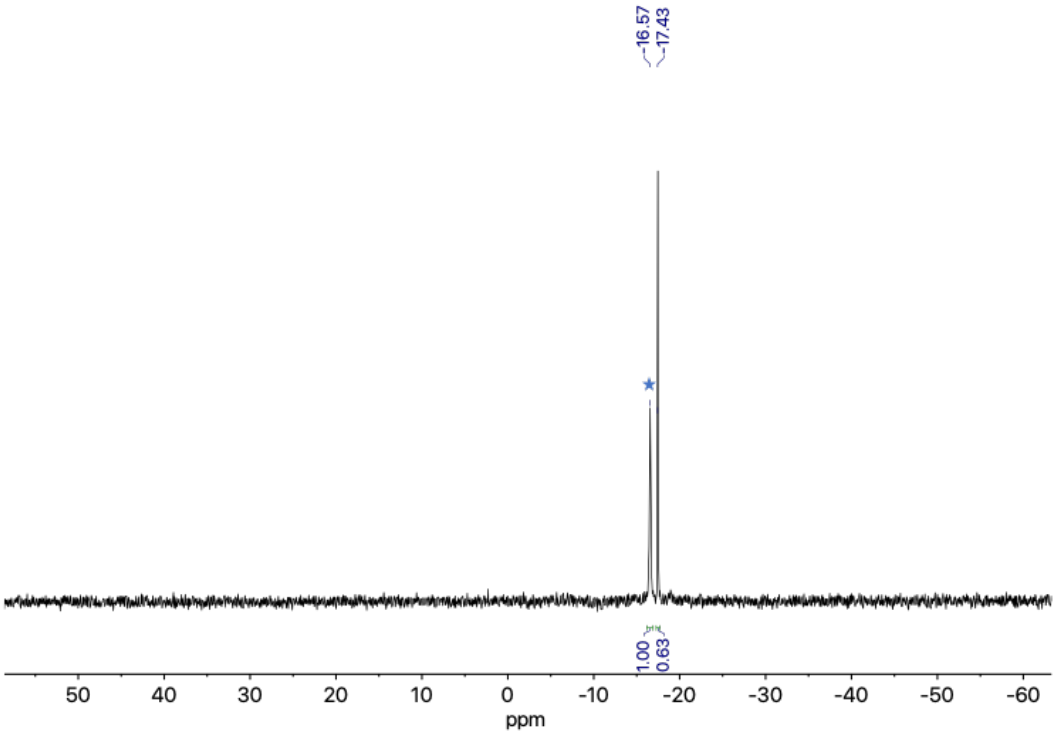

Figure **S30.** $^{31}P\{^{1}H\}$ NMR spectrum of [PNNO]Zn*H* **(4)** (162 MHz, $C_2D_2Cl_4$, 25 °C). Blue star denotes a second species present in solution

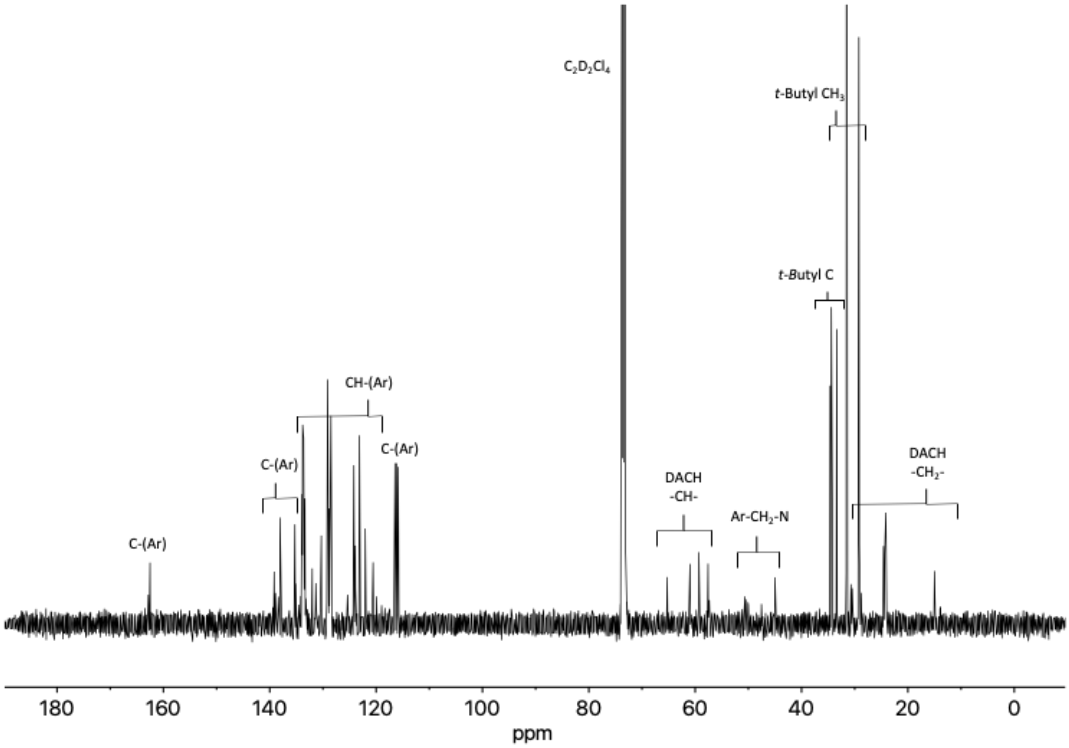

Figure S31. $^{13}C\{^{1}H\}$ NMR spectrum of [PNNO]Zn*H* **(4)** (101 MHz, $C_2D_2Cl_4$, 25 °C).

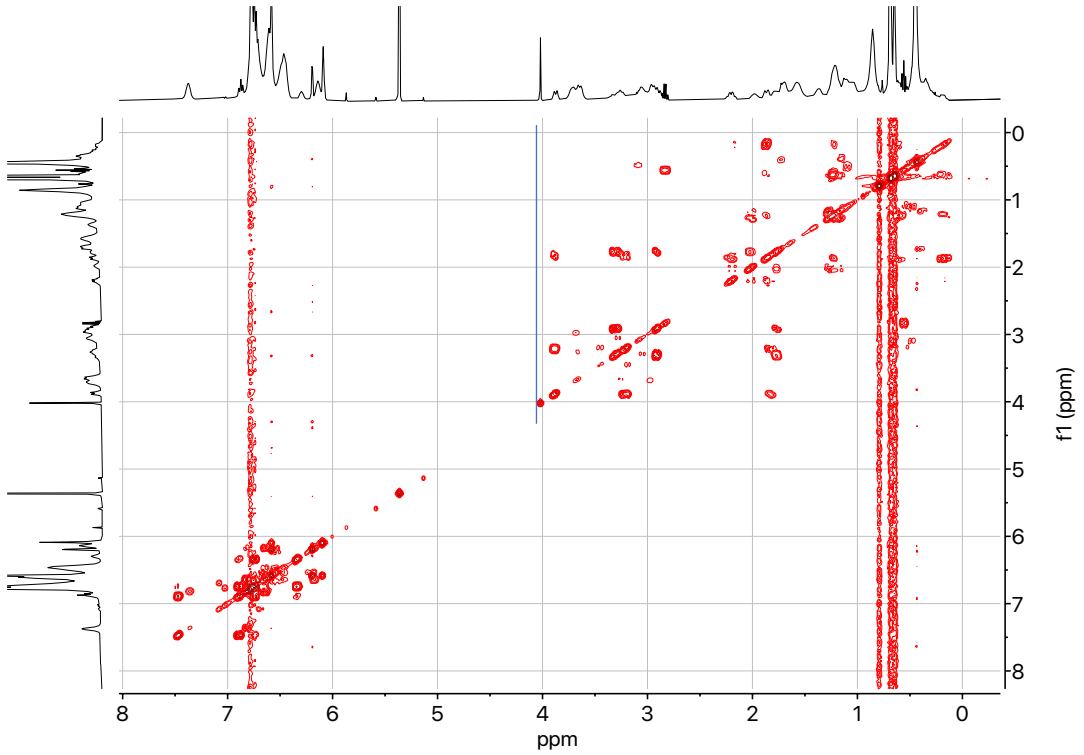

Figure S32. 2D ^{1}H-^{1}H COSY NMR spectrum of [PNNO]Zn*H* **(4)** (400 MHz, $C_2D_2Cl_4$, 25 °C)

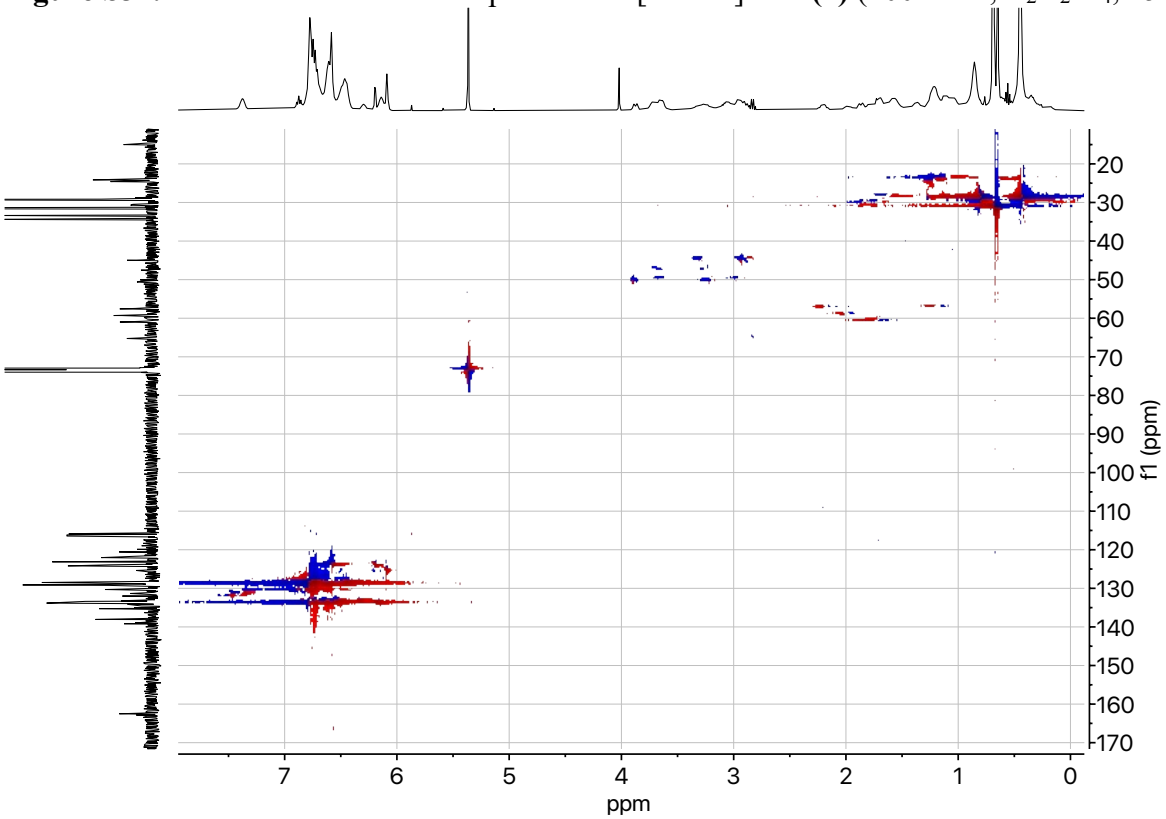

Figure S33. 2D ^{1}H-^{13}C Heteronuclear Single Quantum Coherence (HSQC) NMR spectrum of [PNNO]Zn*H* **(4)** ($C_2D_2Cl_4$, 25 °C).

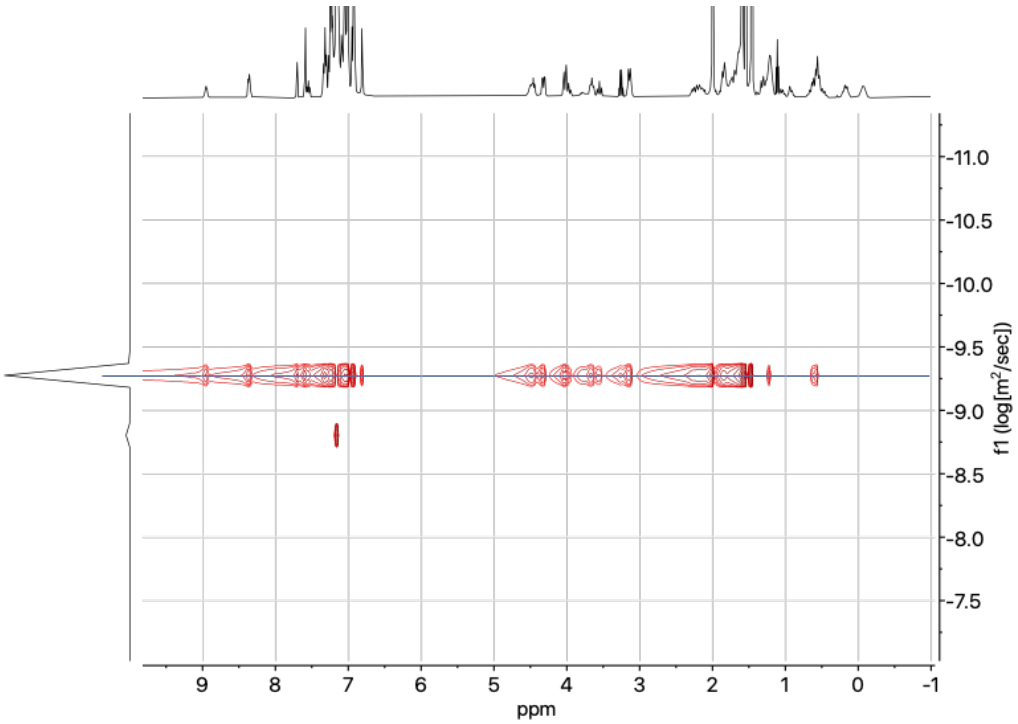

Figure S34. ^{1}H DOSY NMR spectrum of [PNNO]Zn*H* **(4)**in C_6D_6 at 25 °C. The diffusion coefficient is –9.27 log(m^2/sec) or 5.32*10^{-10} m^2/sec, r_h= 5.92 Å.

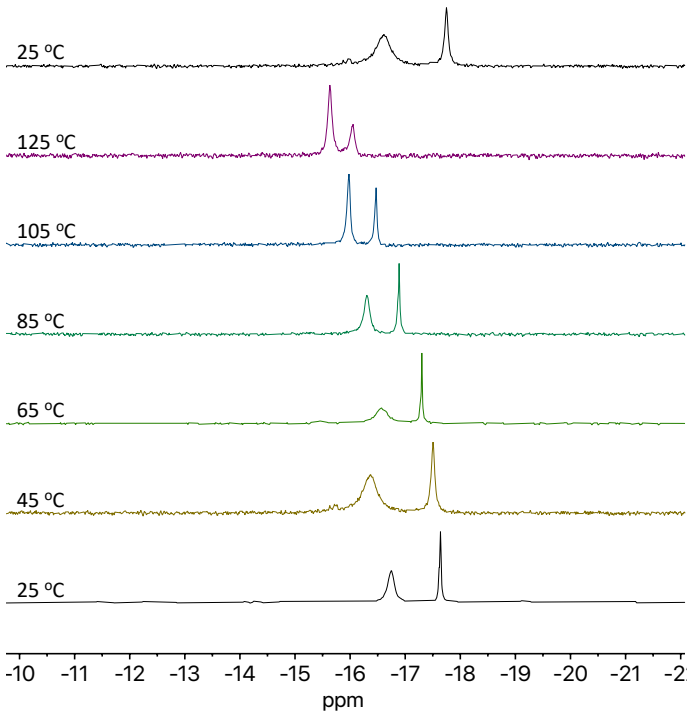

Figure S35. Variable Temperature (VT) ^{31}P{^{1}H} NMR spectra of [PNNO]Zn*H* **(4)** (from 25-125 °C, and from 125-25 °C) (162 MHz, $C_2D_2Cl_4$).

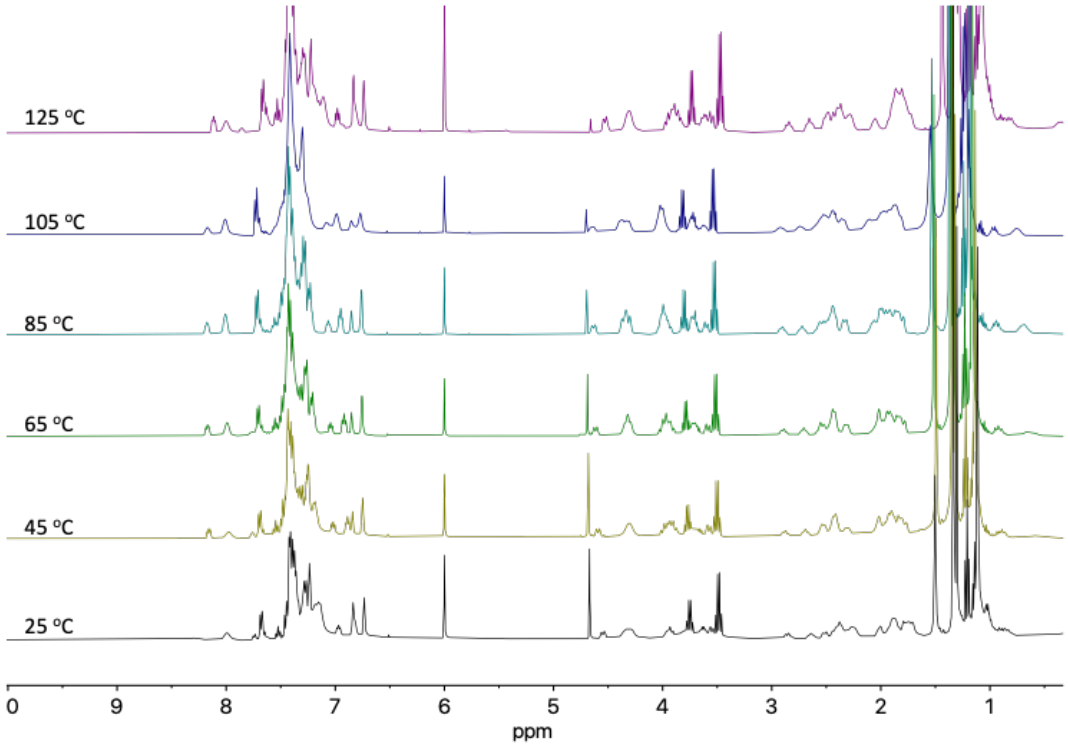

Figure S36. Variable Temperature (VT) ^{1}H NMR spectra of [PNNO]Zn*H* **(4)** (from 25-105 °C, and from 105-25 °C) (400 MHz, D_8-Toluene).

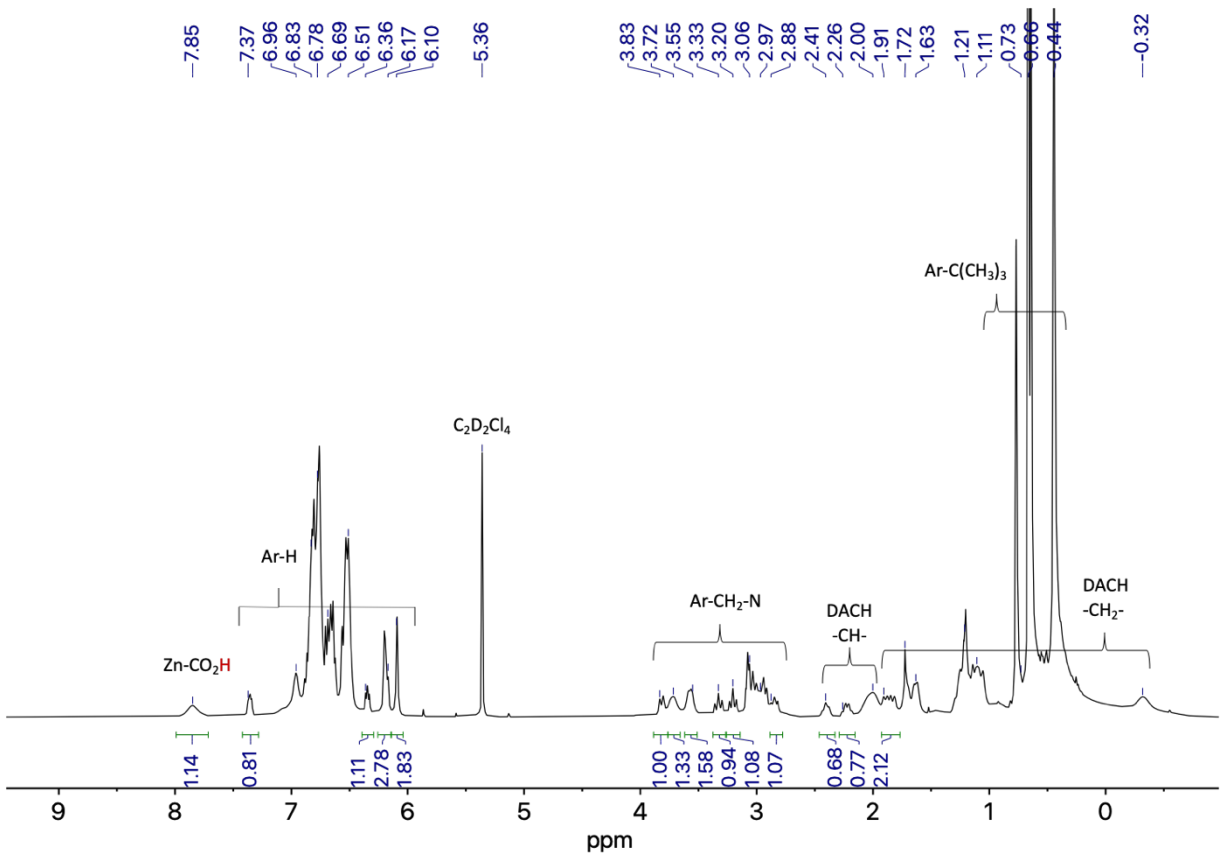

Figure 37. ^{1}H NMR spectrum of [PNNO]Zn(OCOH) **(5)** (400 MHz, $C_2D_2Cl_4$, 25 °C).

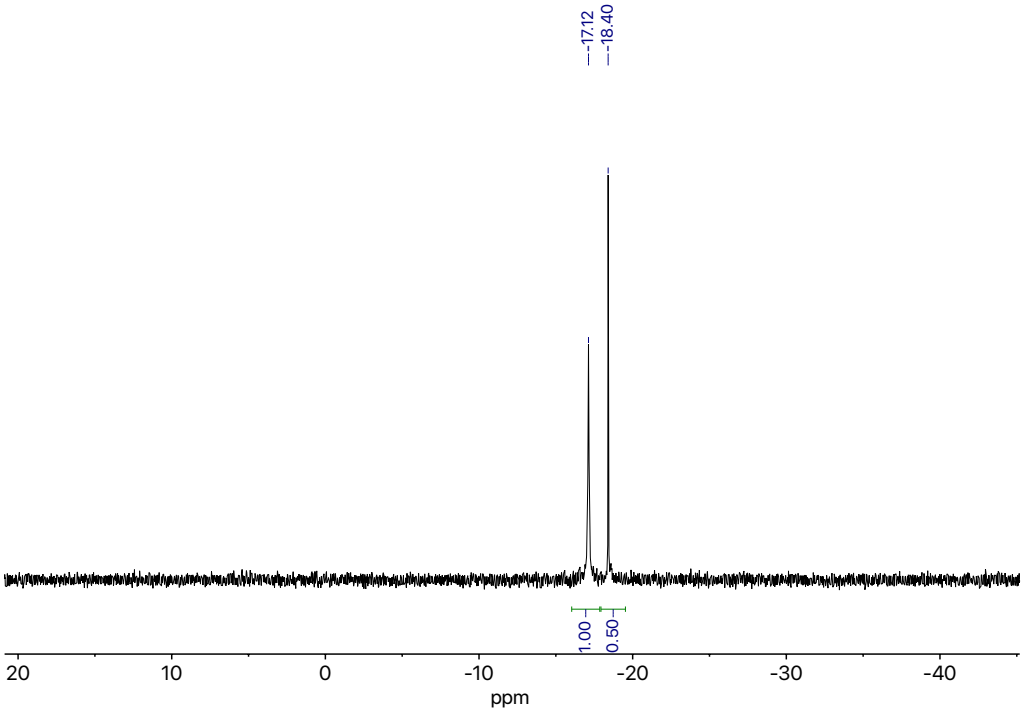

Figure 38. ^{31}P{^{1}H} NMR spectrum of [PNNO]Zn(OCOH) **(5)** (162 MHz, $C_2D_2Cl_4$, 25 °C).

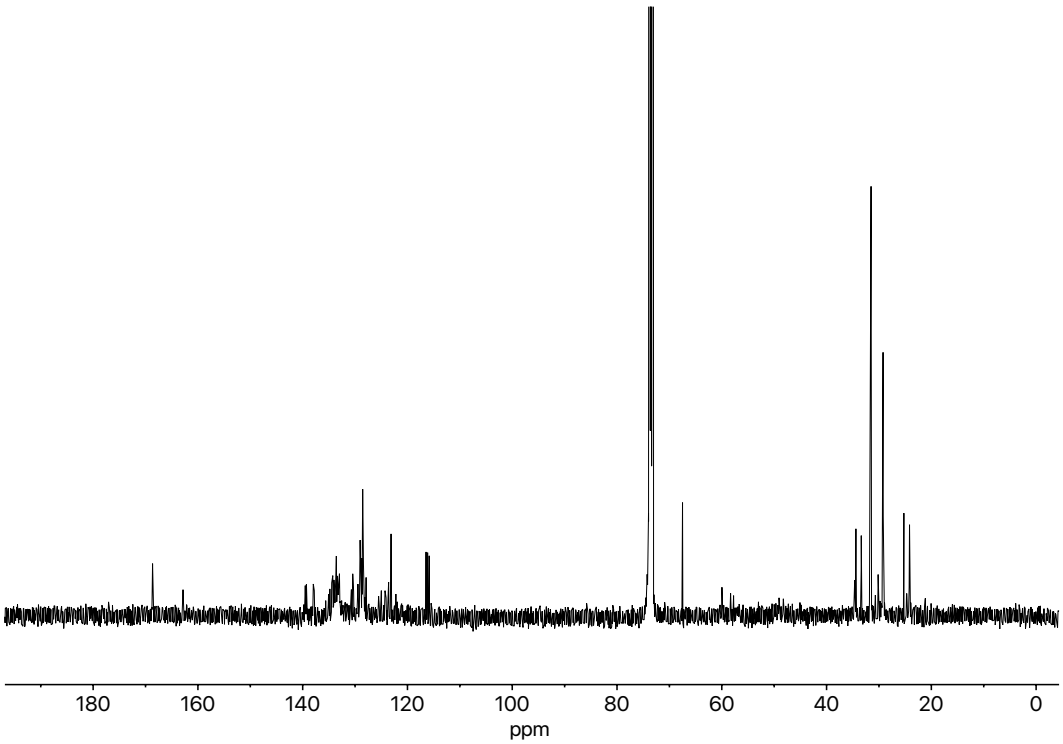

Figure S39. $^{13}C\{^{1}H\}$ NMR spectrum of [PNNO]Zn(OCOH) **(5)** (101 MHz, $C_2D_2Cl_4$, 25 °C).

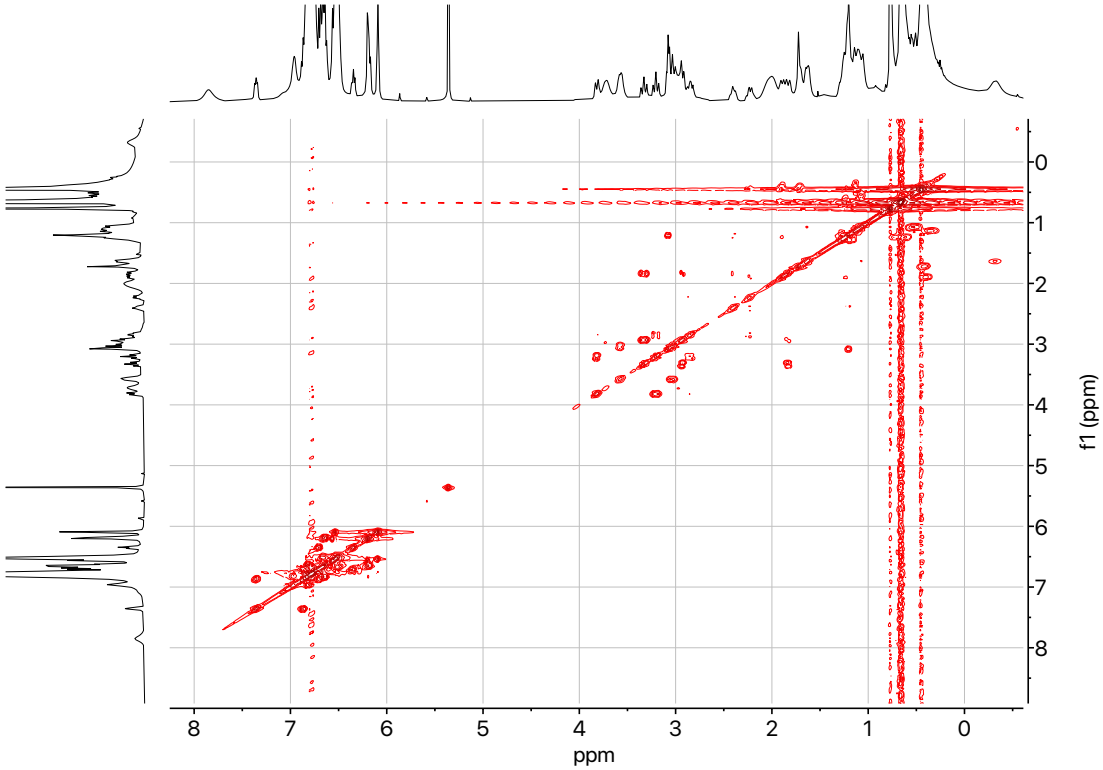

Figure S40. 2D ^{1}H-^{1}H COSY NMR spectrum of [PNNO]Zn(OCOH) **(5)** (400 MHz, $C_2D_2Cl_4$, 25 °C).

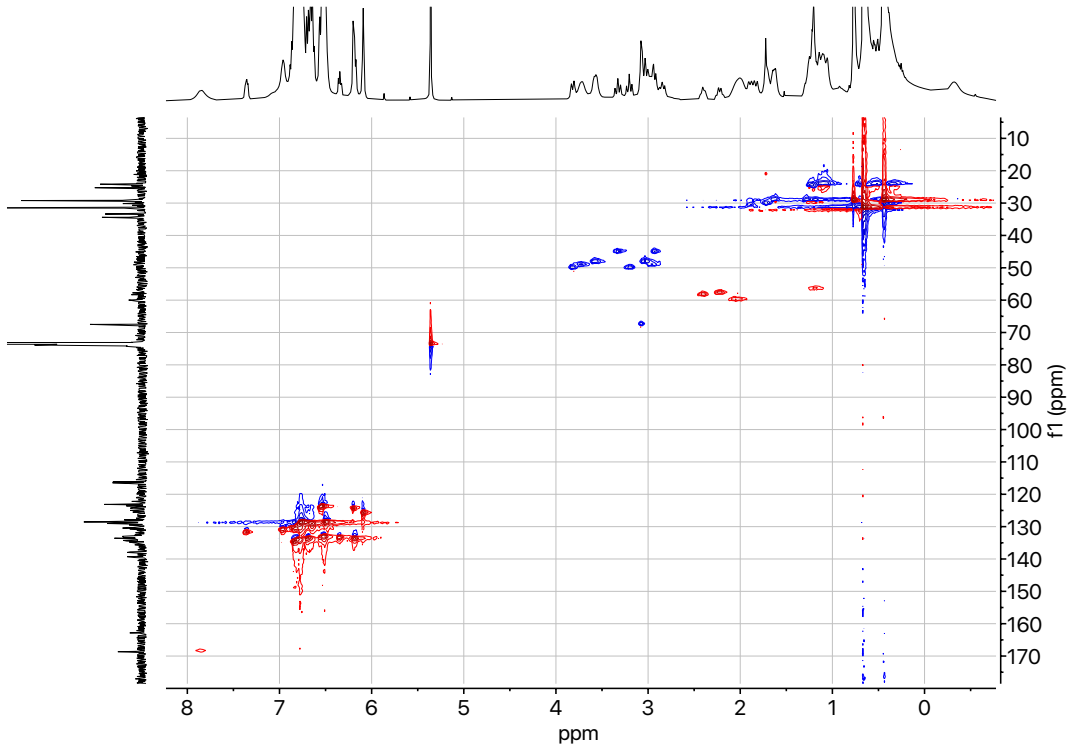

Figure S41. 2D ^{1}H-^{13}C Heteronuclear Single Quantum Coherence (HSQC) NMR spectrum of complex [PNNO]Zn(OCOH) **(5)** ($C_2D_2Cl_4$, 25 °C).

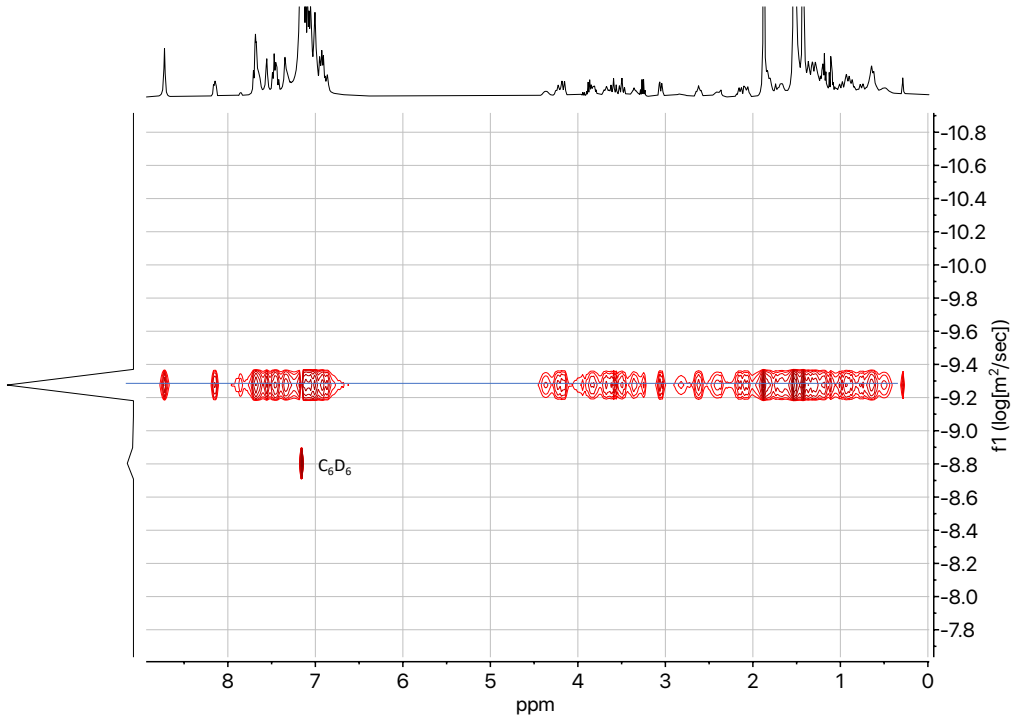

Figure S42. ^{1}H DOSY NMR spectrum of [PNNO]Zn(OCOH) **(5)** in C_6D_6 at 25 °C. The diffusion coefficient is –9.28 log(m^2/sec) or 5.21*10^{-10} m^2/sec, r_h= 6.04 Å.

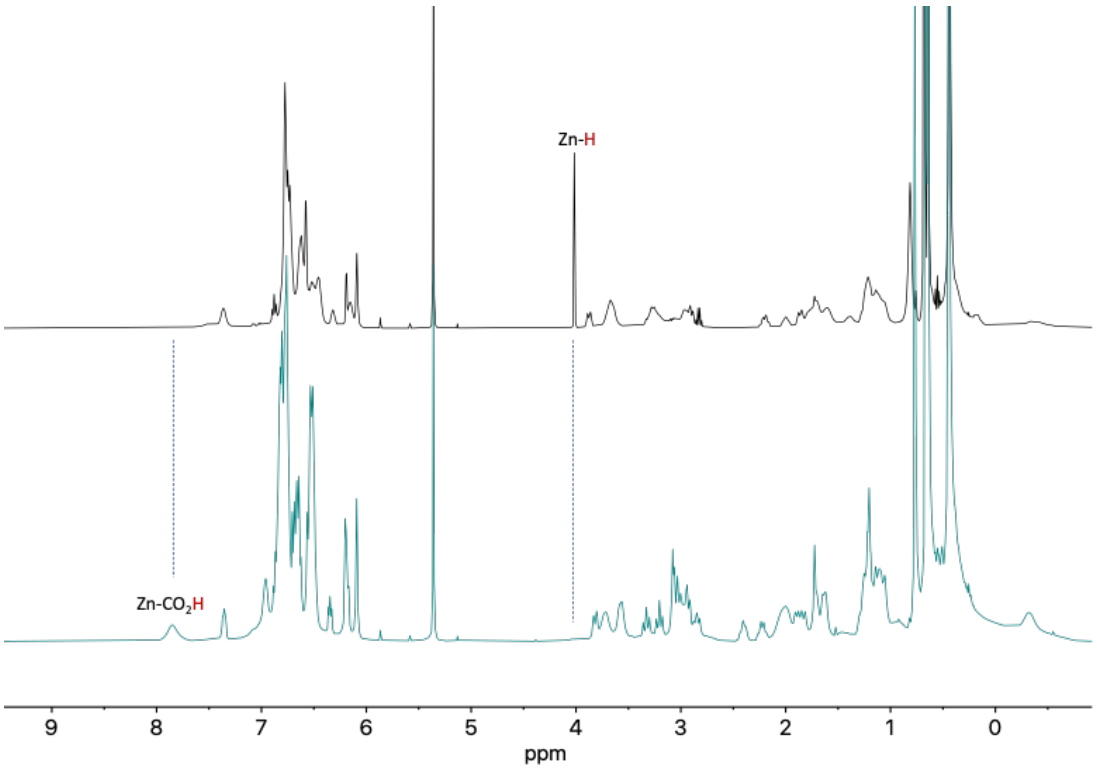

Figure S43. ^{1}H NMR spectra of Zn hydride (top) and zinc formate (bottom) (400 MHz, $C_2D_2Cl_4$, 25 °C).

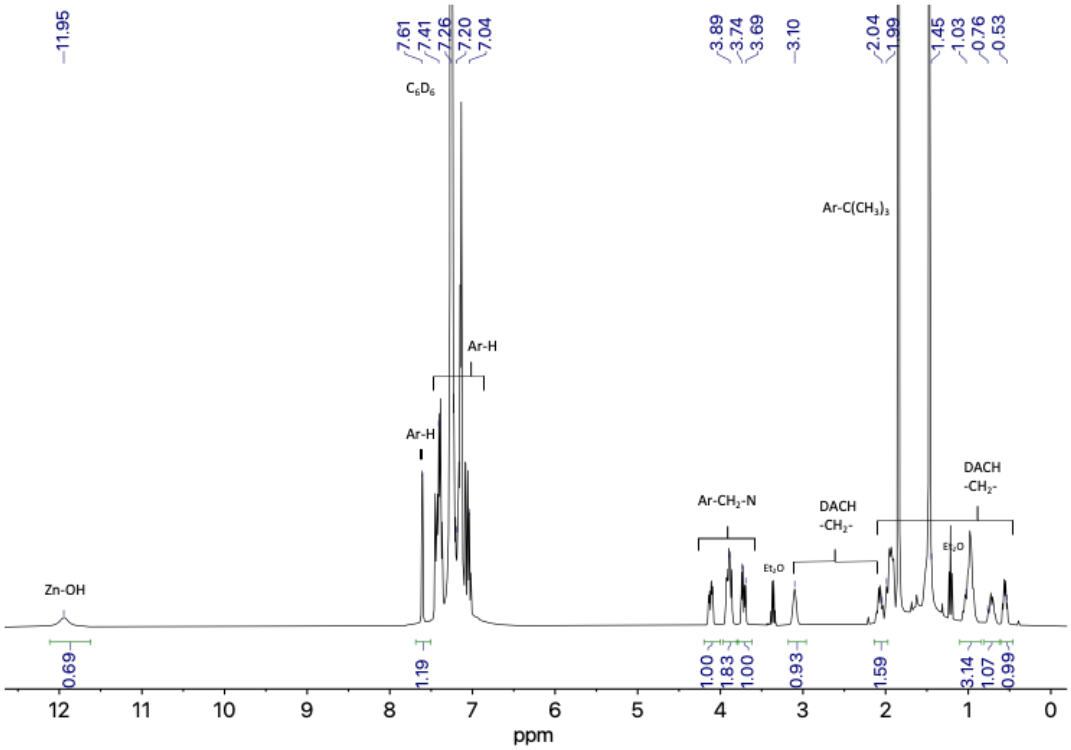

Figure S44. ^{1}H NMR spectrum of [PNNO]ZnOH **(6)** (400 MHz, C_6D_6, 25 °C).

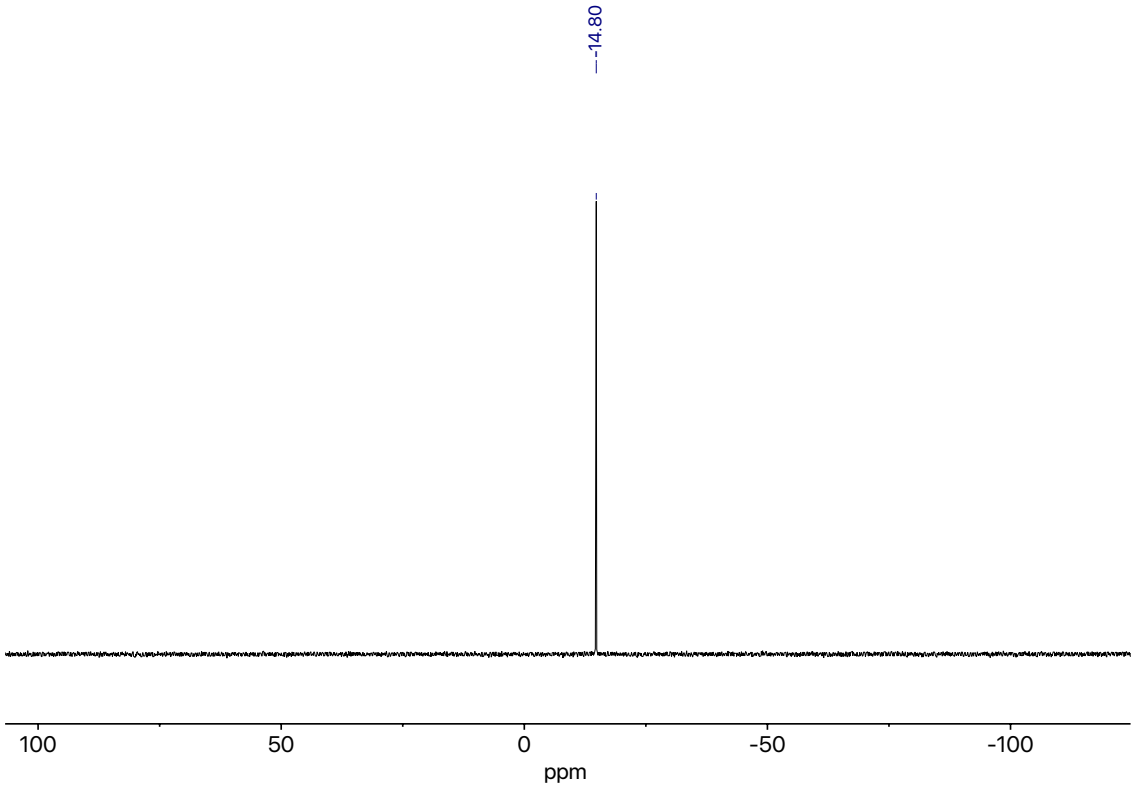

Figure **S45.** $^{31}P\{^{1}H\}$ NMR spectrum of complex **6** LZn-OH (162 MHz, C_6D_6, 25 °C).

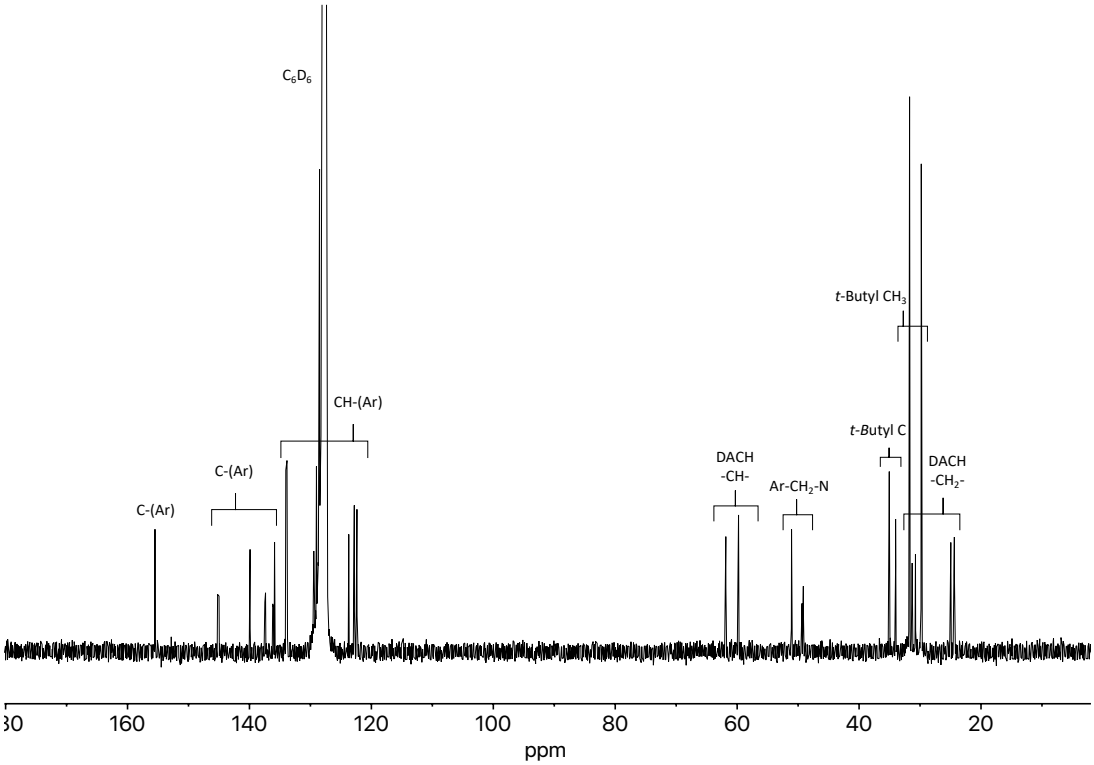

Figure S46. $^{13}C\{^{1}H\}$ NMR spectrum of [PNNO]ZnOH **(6)** (101 MHz, C_6D_6, 25 °C).

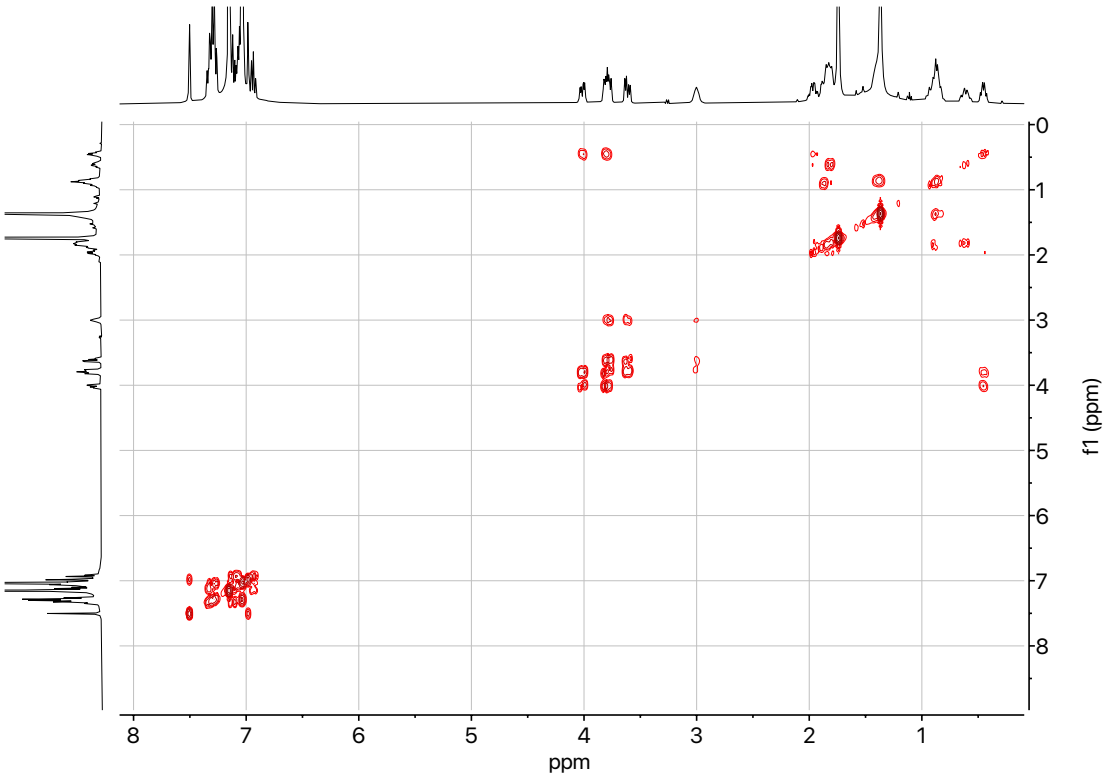

Figure S47. 2D ^{1}H-^{1}H COSY NMR spectrum of [PNNO]ZnOH **(6)** (400 MHz, C_6D_6, 25 °C).

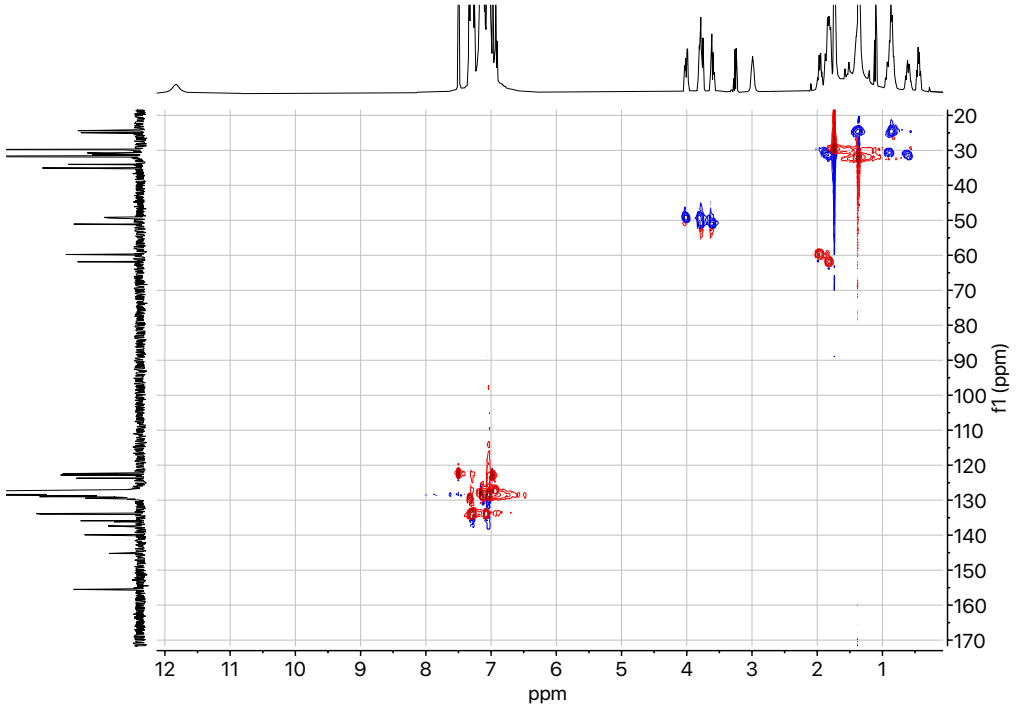

Figure S48. 2D ^{1}H-^{13}C Heteronuclear Single Quantum Coherence (HSQC) NMR spectrum of [PNNO]ZnOH **(6)** (C_6D_6, 25 °C).

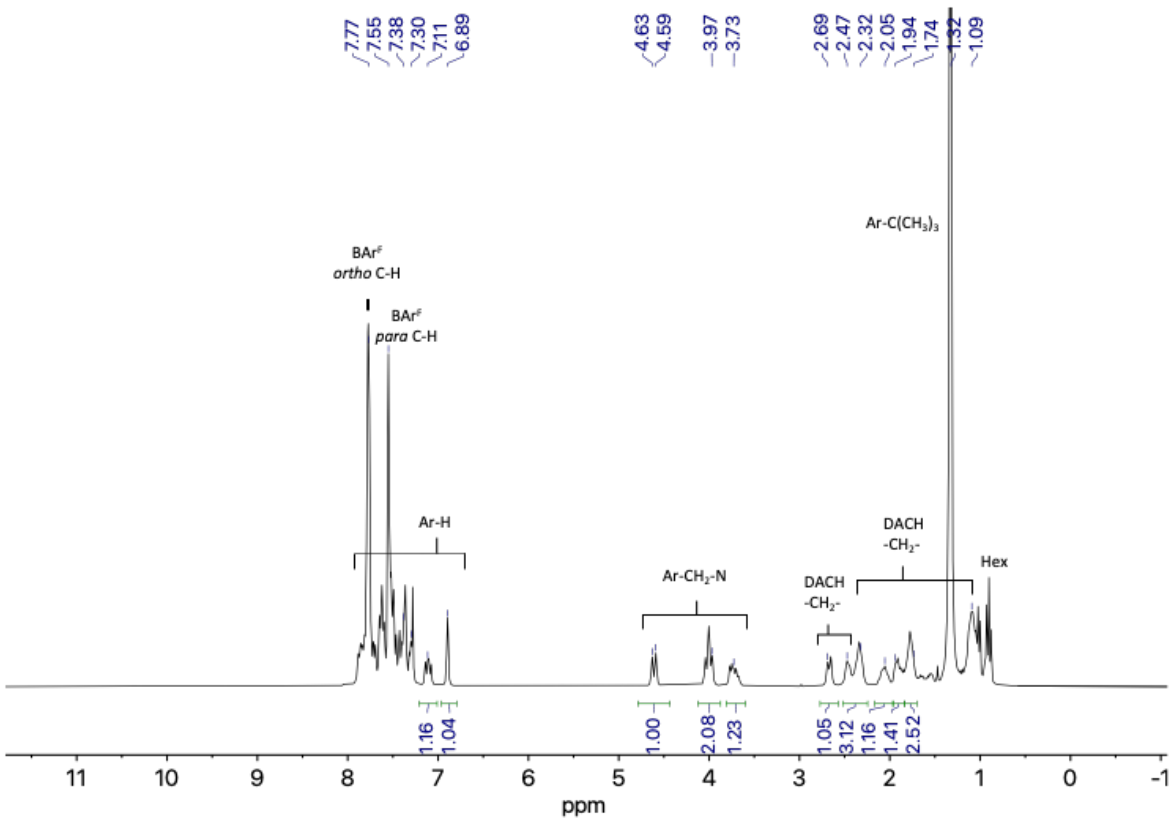

Figure S49. ^{1}H NMR spectrum of complex **2** (400 MHz, $CDCl_3$, 25 °C).

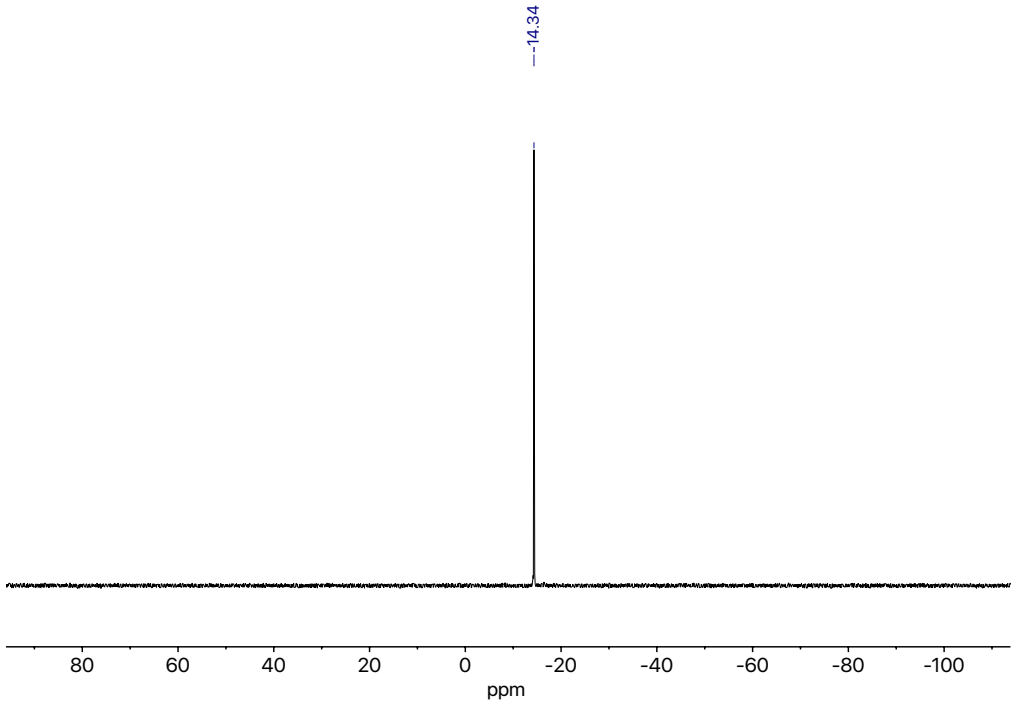

Figure S50. $^{31}P\{^{1}H\}$ NMR spectrum of complex **2** (162 MHz, $CDCl_3$, 25 °C).

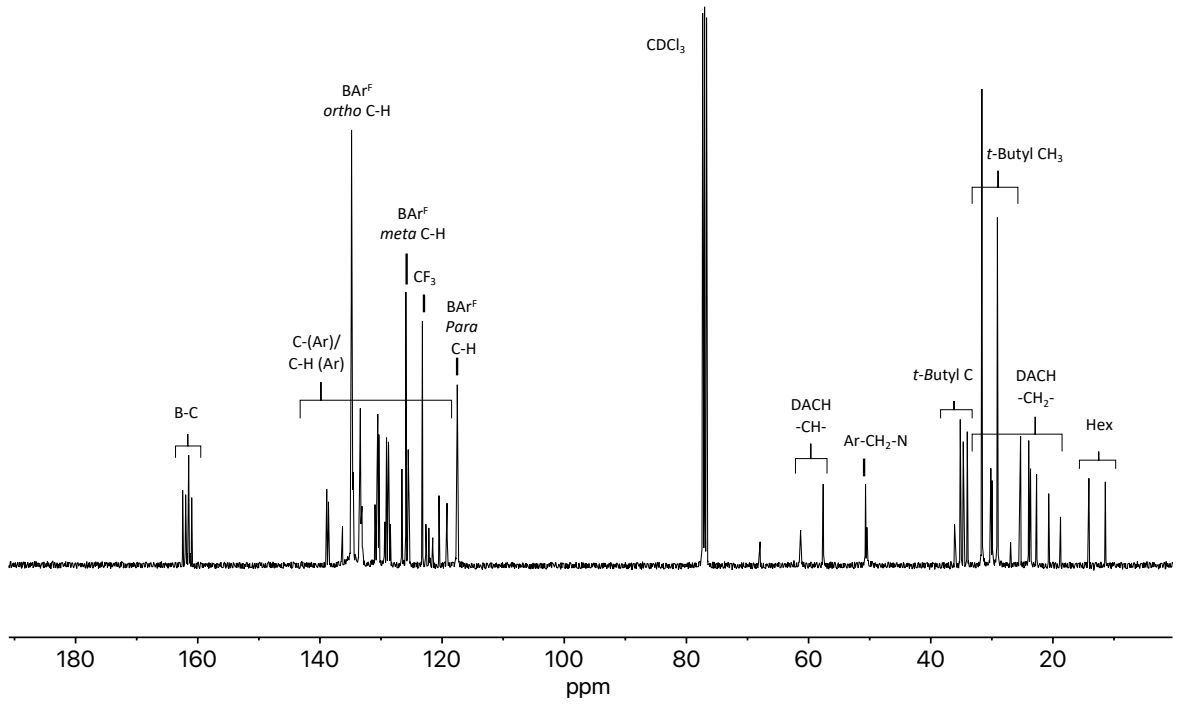

Figure S51. $^{13}C\{^{1}H\}$ NMR spectrum of complex **2** (101 MHz, $CDCl_3$, 25 °C).

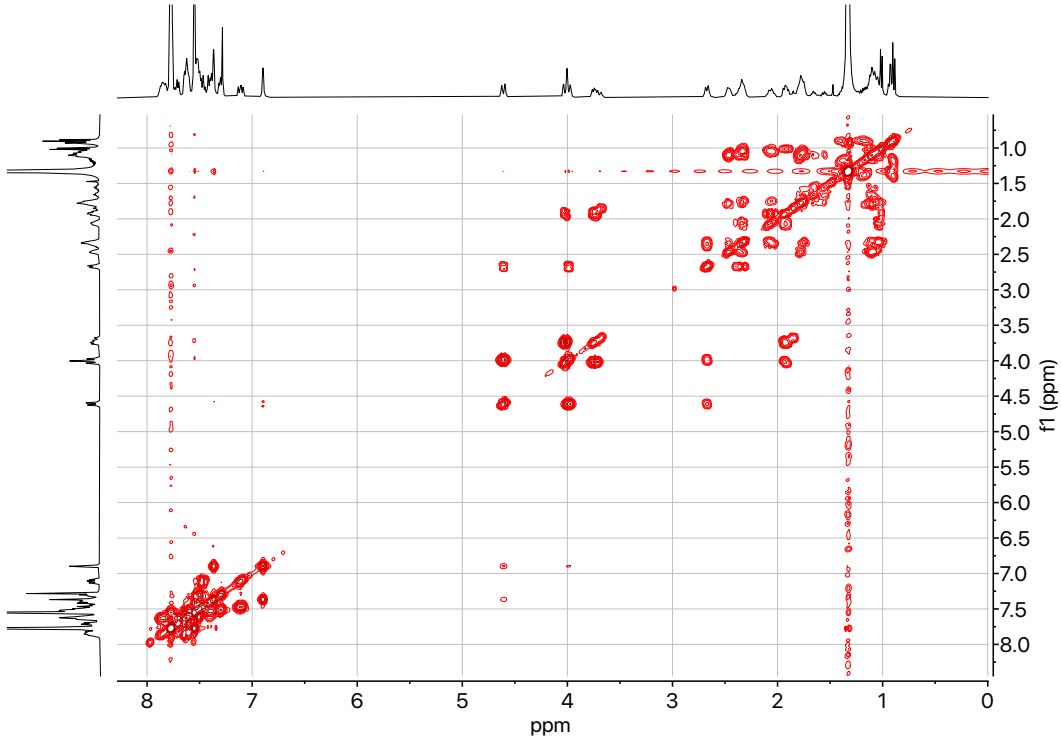

Figure S52. 2D ^{1}H-^{1}H COSY NMR spectrum of complex **2** (400 MHz, $CDCl_3$, 25 °C).

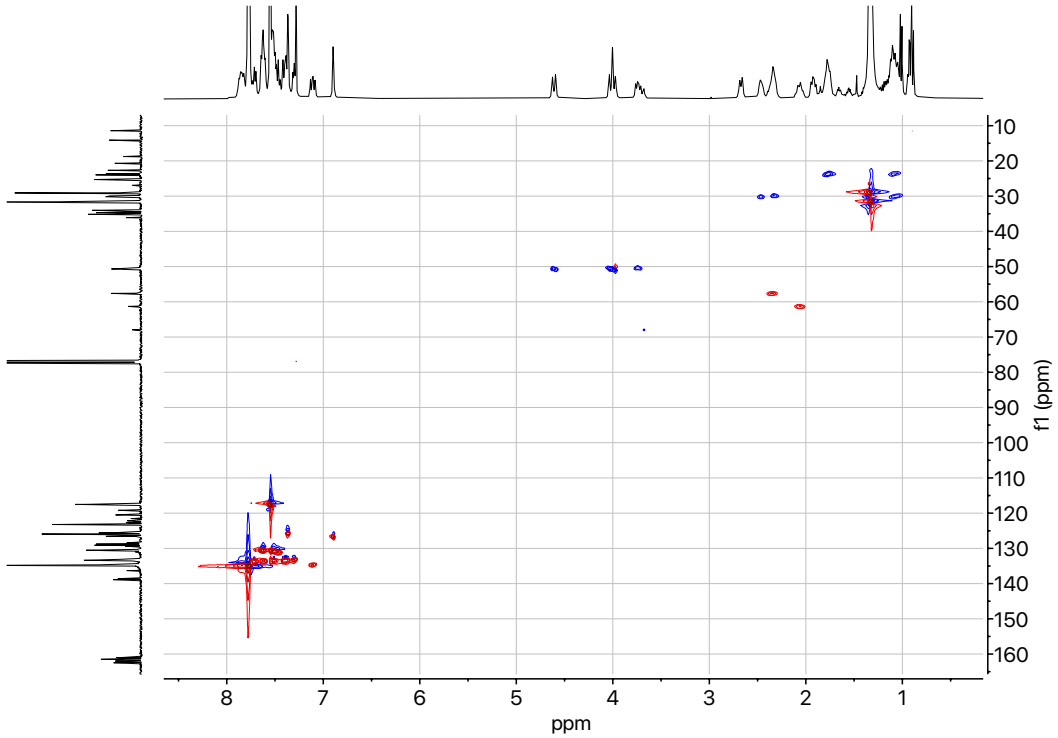

Figure S53. 2D ^{1}H-^{13}C Heteronuclear Single Quantum Coherence (HSQC) NMR spectrum of complex **2** ($CDCl_3$, 25 °C).

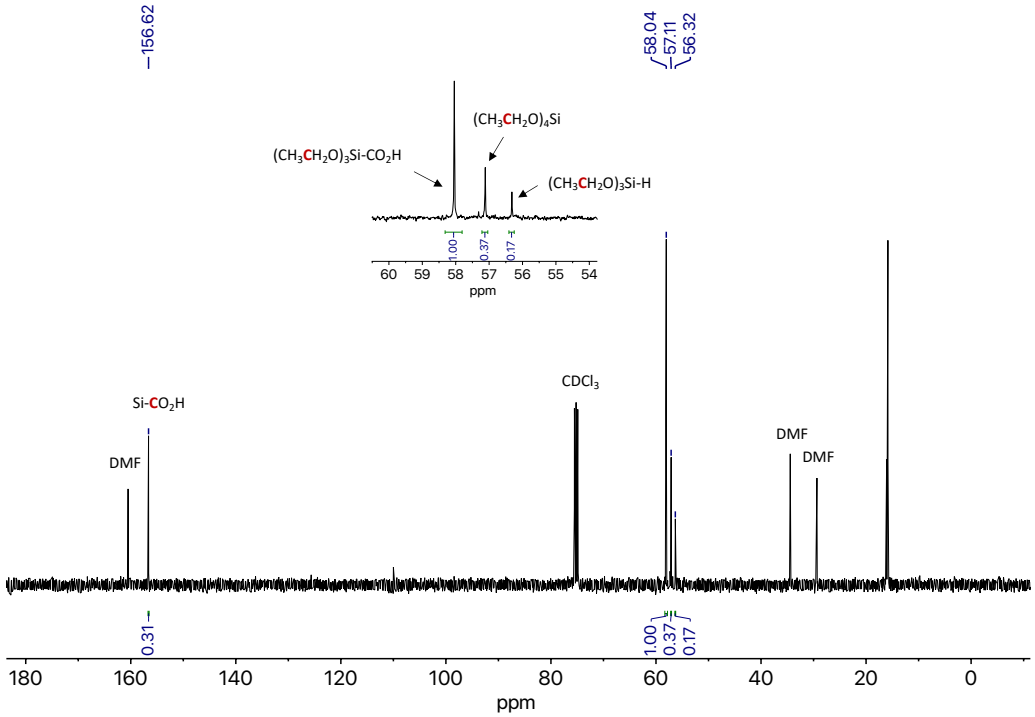

Figure S54. Inverse-gated ^{13}C NMR spectrum of the products of CO_2 hydrosilylation (Table 1, entry 1).

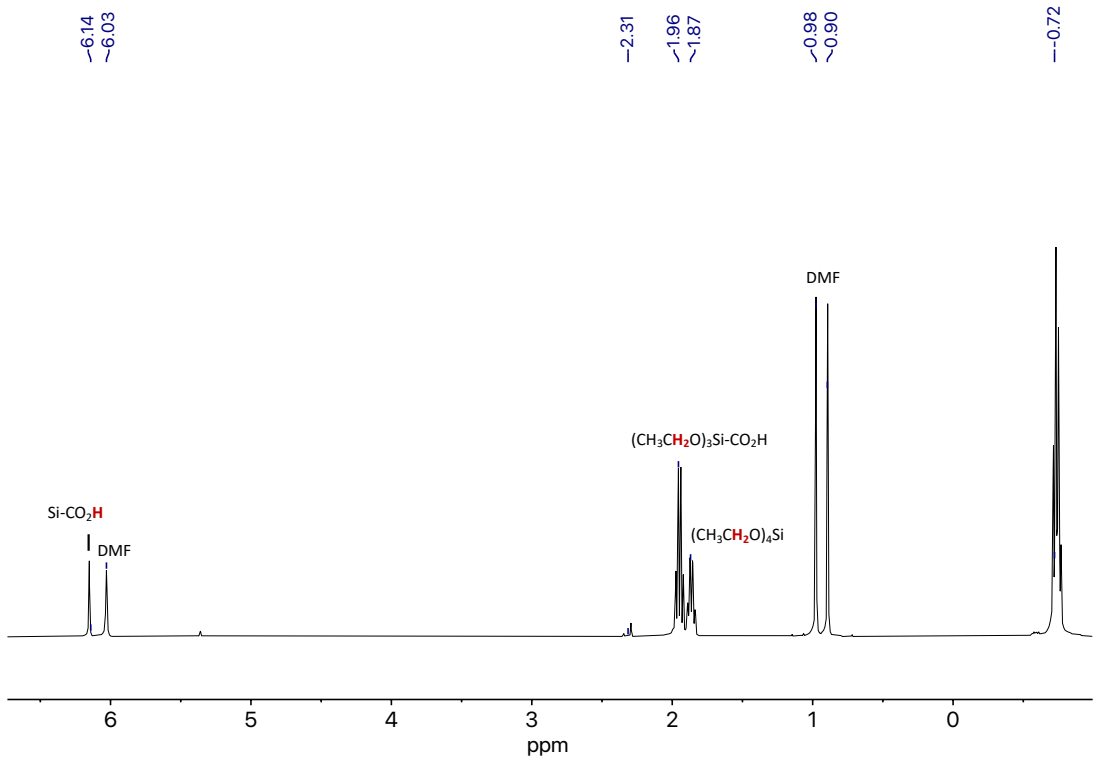

Figure S55. ^{1}H NMR spectrum of the products of CO_2 hydrosilylation (Table 1, entry 1).

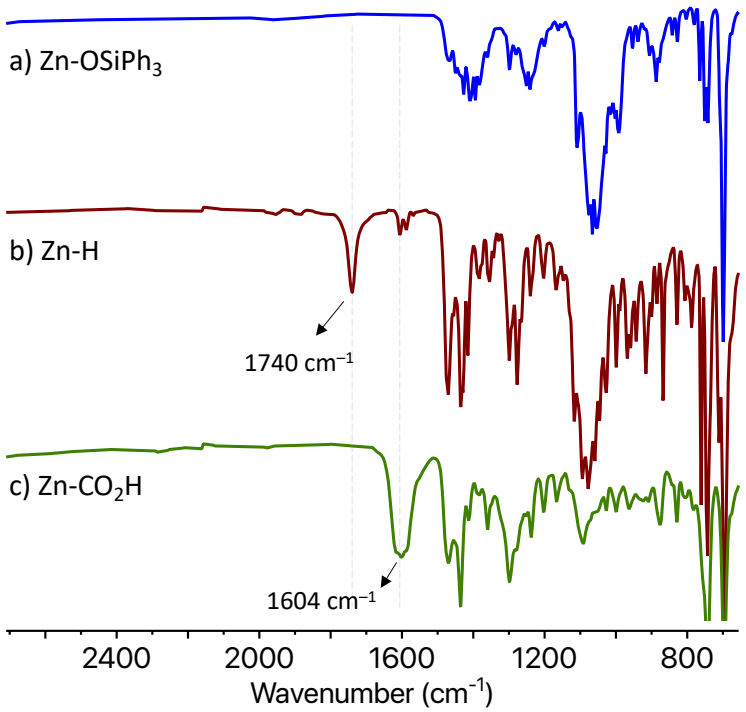

Figure S56. FTIR spectroscopy spectra of a) [PNNO]Zn($OSiPh_3$) (**3**), b) PNNO]ZnH **(4)**, and c) [PNNO]Zn(OCOH) **(5)** complexes.

Proposed mechanism

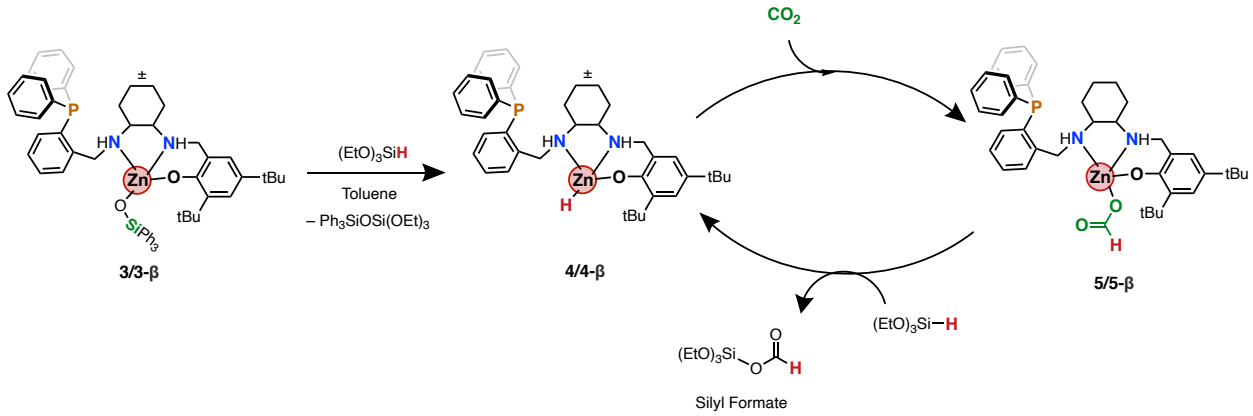

Figure S57. Proposed catalytic cycle for CO_2 hydrosilylation

Based on NMR and FTIR spectroscopy, X-ray crystallography, and reactivity studies, we propose a mechanism for CO_2/hydrosilylation catalyzed by [PNNO]ZnH complex. 1) The [PNNO]Zn($OSiPh_3$) complex reacts with silane to form the [PNNO]ZnH complex (activated catalyst). This is evident by the appearance of a sharp peak at 4.66 ppm in the ^{1}H NMR spectrum and the appearance of a sharp band at 1720 cm^{-1} in the IR spectrum attributed to [PNNO]ZnH46. 2) The [PNNO]ZnH complex reacts readily with CO_2 to form zinc formate species. X-ray crystallography shows the CO_2 coordinates to the zinc center in a monodentate fashion (κ^1-CO_2H). 3) The [PNNO]Zn(OCOH) complex reacts with another molecule of silane to form silyl-formate and generate back the [PNNO]ZnH complex.

Crystal Structures

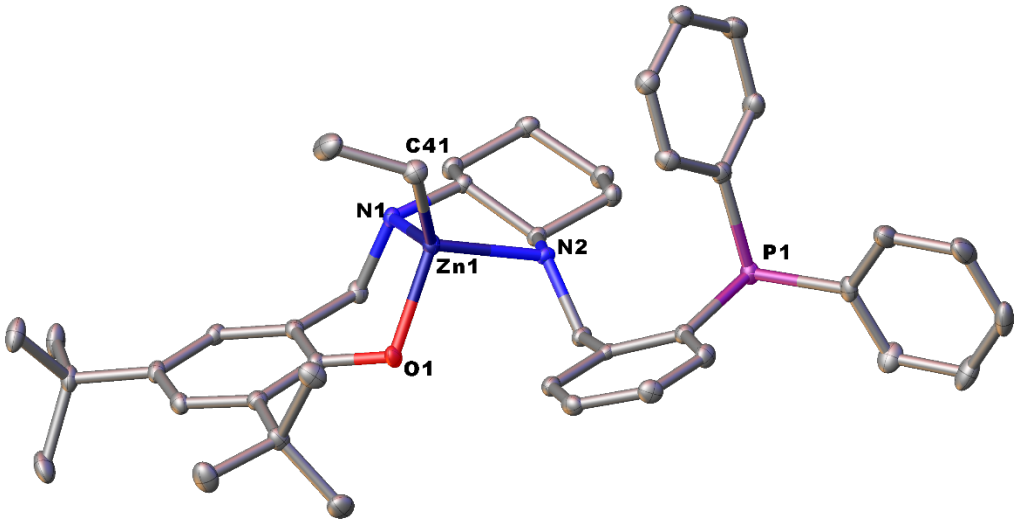

Selected bond length (Å) and angles (°) for [PNNO]Zn(Et) **(1)**.				
Bond Lengths	Zn1-N1	2.1255(13))	Zn1-C41	1.9771(16)
	Zn1-N2	2.1421(13)		
	Zn1-O1	1.9760(12)		
Bond Angles	O1- Zn1-N1	93.63(5)	C41- Zn1-N2	121.64(6)
	O1- Zn1-N2	100.72(5)	N1- Zn1 -N2	83.17(5)
	C41- Zn1-O1	124.47(6)		
	C41- Zn1-N1	123.26(6)		

Figure S54. ORTEP Molecular structure of [PNNO]Zn(Et) **(1)** (depicted with thermal ellipsoids at 50% probability and H atoms, as well as solvent molecules omitted for clarity).

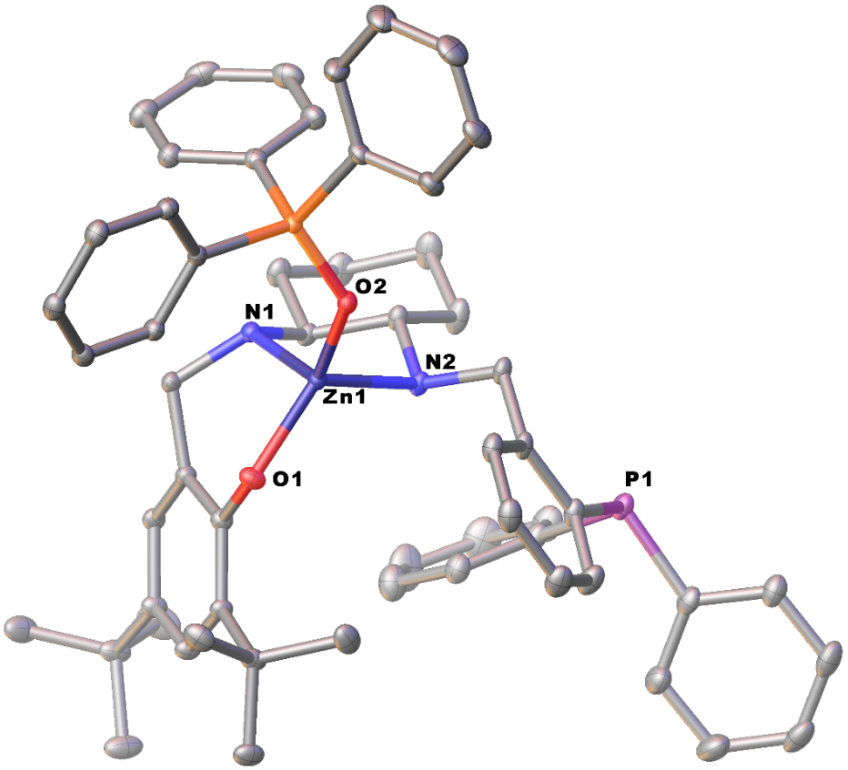

Selected bond length (Å) and angles (°) for [PNNO]Zn(OSiPh$_3$) **(3)**.

Bond Lengths	Zn1-N1	2.0778(11)	Zn1-O2	1.8706(9)
	Zn1-N2	2.1072(11)		
	Zn1-O1	1.8983(10)		
Bond Angles	O1- Zn1-N1	98.04(4)	O2- Zn1-N2	105.87(4)
	O1- Zn1-N2	119.34(4)	N1- Zn1 -N2	84.64(4)
	O2- Zn1-O1	124.87(4)		
	O2- Zn1-N1	116.89(4)		

Figure S55. ORTEP Molecular structure of [PNNO]Zn(OSiPh$_3$) **(3)** (depicted with thermal ellipsoids at 50% probability and H atoms, minor disorders as well as solvent molecules omitted for clarity).

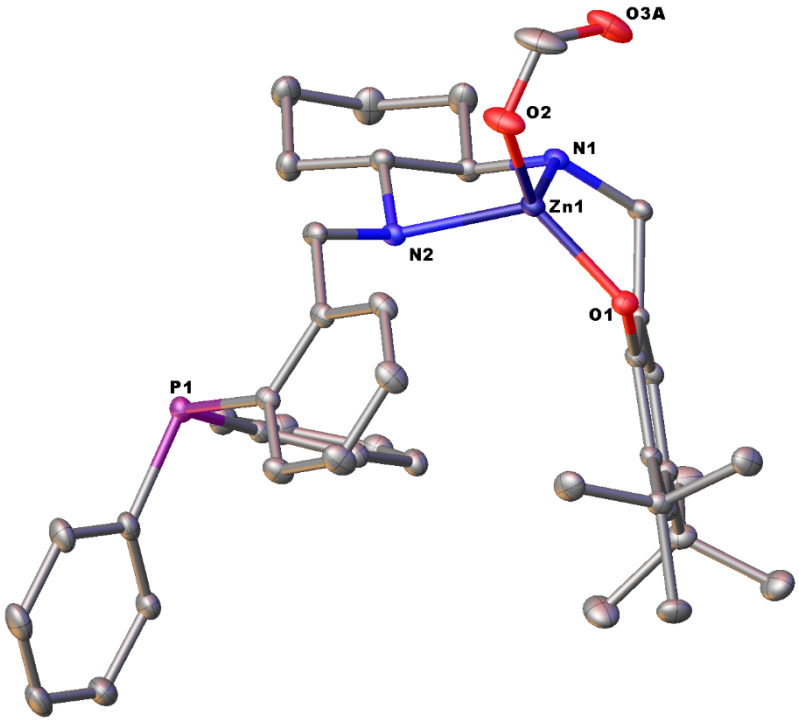

Selected bond length (Å) and angles (°) for [PNNO]Zn(OCOH) **(4)**.				
Bond Lengths	Zn1-N1	2.0484(10)	Zn1-O2	1.9488(10)
	Zn1-N2	2.1233(11)		
	Zn1-O1	1.8941(9)		
Bond Angles	O1- Zn1-N1	99.73(4)	O2- Zn1-N2	100.28(4)
	O1- Zn1-N2	120.63(4)	N1- Zn1 -N2	84.52(4)
	O2- Zn1-O1	123.15(4)		
	O2- Zn1-N1	123.44(4)		

Figure S56. ORTEP Molecular structure of [PNNO]Zn(OCOH) **(4)** (depicted with thermal ellipsoids at 50% probability and H atoms, as well as solvent molecules omitted for clarity).
Table S1. Selective crystal data for complexes **1-3**.

	[PNNO]Zn(Et) **(1)**	[PNNO]Zn(OSiPh$_3$) **(3)**	[PNNO]Zn(OCOH) **(4)**
Identification code	Pm295	mo_pm291_0m	mo_pm294_0m
Empirical formula	$C_{42}H_{55}N_2OPZn$	$C_{126}H_{154}N_4O_5P_2Si_2Zn_2$	$C_{41}H_{51}N_2O_3PZn$
Formula weight	700.22	2053.38	716.17
Temperature/K	90	90	90
Crystal system	monoclinic	triclinic	triclinic
Space group	$P2_1/n$	P-1	P-1
a/Å	8.0842(8)	11.048(2)	9.8580(13)
b/Å	23.079(2)	14.012(3)	13.1069(17)
c/Å	20.076(2)	19.725(4)	15.788(2)
α/°	90	80.978(7)	72.988(3)
β/°	92.997(3)	87.207(6)	75.997(3)
γ/°	90	69.507(6)	83.549(3)
Volume/Å^3	3740.5(6)	2824.8(11)	1890.8(4)
Z	4	1	2
ρ_{calc}g/cm^3	1.243	1.207	1.258
μ/mm^{-1}	0.733	0.529	0.731
F(000)	1496.0	1096.0	760.0
Crystal size/mm^3	0.2 × 0.12 × 0.09	0.23 × 0.16 × 0.1	0.12 × 0.1 × 0.09
Radiation	MoKα (λ = 0.71073)	MoKα (λ = 0.71073)	MoKα (λ = 0.71073)
2Θ range for data collection/°	2.69 to 56.652	2.09 to 61.438	3.252 to 66.66
Index ranges	? ≤ h ≤ ?, ? ≤ k ≤ ?, ? ≤ l ≤ ?	-15 ≤ h ≤ 15, -20 ≤ k ≤ 19, -27 ≤ l ≤ 28	-15 ≤ h ≤ 15, -20 ≤ k ≤ 20, -23 ≤ l ≤ 24
Reflections collected	9288	64816	74995
Independent reflections	9288[R_{int}=0.0435, R_{sigma}= 0.0349]	17360 [R_{int} = 0.0398, R_{sigma} = 0.0353]	14497 [Rint = 0.0398, R_{sigma} = 0.0319]
Data/restraints/parameters	9288/0/431	17360/147/699	14497/1/449
Goodness-of-fit on F^2	1.032	1.038	1.020
Final R indexes [I>=2σ (I)]	R_1 =0.0363, wR_2 = 0.0724	R_1 = 0.0371, wR_2 = 0.1024	R_1 = 0.0363, wR_2 = 0.0877
Final R indexes [all data]	R_1 = 0.0515, wR_2 = 0.0768	R_1 = 0.0424, wR_2 = 0.1063	R_1 = 0.0500, wR_2 = 0.0949
Largest diff. peak/hole / e Å^{-3}	0.36/-0.34	0.98/-0.67	1.23/-0.63

[a] $R_1 = \Sigma ||F_o| - |F_c|| / \Sigma |F_o|$. [b] $wR_2 = [\Sigma (w (F_o^2 - F_c^2)^2) / \Sigma w(F_o^2)_2]^{1/2}$

References

1. Krause, L.; Herbst-Irmer, R.; Sheldrick, G. M.; Stalke, D., Comparison of silver and molybdenum microfocus X-ray sources for single-crystal structure determination. *J. Appl. Crystallogr.* **2015,** *48* (1), 3-10.
2. Sheldrick, G. M., SHELXT–Integrated space-group and crystal-structure determination. *Acta Crystallogr., Sect. A: Found. Crystallogr.* **2015,** *71* (1), 3-8.
3. Sheldrick, G. M., Crystal structure refinement with SHELXL. *Acta Crystallographica Section C: Structural Chemistry* **2015,** *71* (1), 3-8.
4. Dolomanov, O. V.; Bourhis, L. J.; Gildea, R. J.; Howard, J. A. K.; Puschmann, H., OLEX2: a complete structure solution, refinement and analysis program. *J. Appl. Crystallogr.* **2009,** *42* (2), 339-341.
5. Palmer, D., CrystalMaker. *Begbroke, Oxfordshire, England: CrystalMaker Software Ltd* **2014**.
6. Jung, H.-J.; Chang, C.; Yu, I.; Aluthge, D. C.; Ebrahimi, T.; Mehrkhodavandi, P., Coupling of Epoxides and Lactones by Cationic Indium Catalysts To Form Functionalized Spiro-Orthoesters. *ChemCatChem* **2018,** *10* (15), 3219-3222.
7. Labourdette, G.; Lee, D. J.; Patrick, B. O.; Ezhova, M. B.; Mehrkhodavandi, P., Unusually stable chiral ethyl zinc complexes: Reactivity and polymerization of lactide. *Organometallics* **2009,** *28* (5), 1309-1319.
8. Baalbaki, H. A.; Nyamayaro, K.; Shu, J.; Goonesinghe, C.; Jung, H. J.; Mehrkhodavandi, P., Indium-Catalyzed CO_2/Epoxide Copolymerization: Enhancing Reactivity with a Hemilabile Phosphine Donor. *Inorg. Chem.* **2021,** *60*, 19304-19314.
9. Baalbaki, H. A.; Nyamayaro, K.; Shu, J.; Goonesinghe, C.; Jung, H. J.; Mehrkhodavandi, P., Indium-Catalyzed CO_2/Epoxide Copolymerization: Enhancing Reactivity with a Hemilabile Phosphine Donor. *Inorg. Chem.* **2021,** *60* (24), 19304-19314.
10. Saravanan, A.; Vo, D.-V. N.; Jeevanantham, S.; Bhuvaneswari, V.; Narayanan, V. A.; Yaashikaa, P. R.; Swetha, S.; Reshma, B., A comprehensive review on different approaches for CO_2 utilization and conversion pathways. *Chem. Eng. Sci.* **2021,** *236*, 116515.
11. Caytan, E.; Remaud, G. S.; Tenailleau, E.; Akoka, S., Precise and accurate quantitative ^{13}C NMR with reduced experimental time. *Talanta* **2007,** *71* (3), 1016-1021.
12. Dixon, J. A.; Schiessler, R. W., Viscosities of benzene-d6 and cyclohexane-d12. *J. Phys. Chem.* **1954,** *58* (5), 430-432.